ChemComm

COMMUNICATION

# Thioamide-based Fluorescent Sensors for Dipeptidyl Peptidase 4

Hoang Anh T. Phan,[a] Yanan Chang,[a] Samuel A. Eaton,[a] E. James Petersson[a,b]*

Received 00th January 20xx,
Accepted 00th January 20xx

DOI: 10.1039/x0xx00000x

**Dipeptidyl peptidase 4 (DPP-4) is a promising biomarker for cancer and metabolic diseases. We demonstrate the design of novel fluorescent DPP-4 probes based on the protease's native substrates using a thioamide as a quencher for measuring *in vitro* kinetics, inhibition with sitagliptin, and DPP-4 activity in saliva samples.**

Dipeptidyl peptidase 4 (DPP-4) is a serine protease that preferably cleaves at a proline or an alanine at the second amino acid of its substrates, liberating dipeptides.[1] Interestingly, DPP-4 is a multifunctional protein also known as CD26, which serves as T cell costimulatory receptor in addition to its enzymatic activity.[2] When DPP-4 was first discovered by Hopsu-Havu and Glenner in 1966, it was initially called glycyl-proline naphthylamidase due to the fact that it could cleave the substrate glycyl-DL-prolyl-β-naphthylamide (GP-βNA).[3] DPP-4 can inactivate peptides whose N-termini are important for biological function or cleave peptides to generate new ones.[4, 5]

Among the natural substrates of DPP-4 are the peptides from the pituitary adenylate cyclase-activating polypeptide (PACAP)/glucagon family such as glucagon-like polypeptide 1 (GLP-1) and gastric inhibitory polypeptide (GIP), which are important in regulating glucose homeostasis.[4, 6] GLP-1 stimulates insulin release, but it can be rapidly cleaved by DPP-4 with a half-life of less than 2 minutes. There have been major advances in DPP-4-based therapeutics for treatment of diabetes, especially in creating stabilized GLP-1 analogs and DPP-4 inhibitors such as sitagliptin (Januvia).[7-10] Beyond GLP-1, DPP-4 cleaves a diverse repertoire of bioactive peptides, such as vasoactive intestinal peptide (VIP), substance P, pancreatic polypeptide (PP), peptide YY (PYY), and neuropeptide Y (NPY). DPP-4 is expressed in different tissues as either an anchored transmembrane protease or a soluble circulating one, and its anomalous activity has also been linked to cancer (solid tumors), hematological malignancies, immune diseases, and infectious diseases.[4, 5] Studies have identified DPP-4 as a promising biomarker for early diagnosis and treatment of diseases such as lung diseases, diabetic kidney disease,[11] rheumatoid arthritis,[12] post-kidney transplant tubulitis,[12] and liver disease.[13] There is thus a need to develop probes to monitor DPP-4 activity real-time.

Common chromogenic substrates for DPP-4 include GP-βNA,[3] Ala-Pro-7-amino-4-trifluoromethyl-coumarin (AP-AFC), and Gly-Pro-7-amido-4-methylcoumarin (GP-AMC). Many DPP-4 probes utilize a pro-fluorophore Forster resonance energy transfer (FRET), photoinduced electron transfer (PeT), or intramolecular charge transfer (ICT) approach where the fluorophore is quenched when conjugated to a short recognition dipeptide (*e.g.,* Gly-Pro; Ala-Pro), and can return to its highly emissive state upon cleavage by the protease.[14-17] These strategies can perturb and compromise the recognition sequences, thereby preventing accurate reporting of proteolysis. For instance, in ICT-based probes GP-βNA, AP-AFC, and GP-AMC, the chromophore is attached directly to the cleavage site so no information can be gained on the C terminal side (called the prime side) of the cleavage site. Even the N-terminal (non-prime) side information can be compromised. A study showed that P1 substitution in the P2-P1-AMC probes did not reflect mutation effects observed in the full-length peptide substrates of DPP-4.[18] Additionally, an approach utilizing FRET pairs, that require labeling on either side of the scissile bond, is not compatible with monitoring aminopeptidases or carboxypeptidases where recognition of the amino acid at the substrate terminus is essential.

Our laboratory has previously shown that thioamides can quench donor fluorophores such as tryptophan, tyrosine, fluorescein, acridonylalanine, and 7-methoxycoumarin, serving as a minimally perturbing probe for protein dynamics and proteolysis.[19-23] For the general design, we typically incorporate

[a] *Department of Chemistry, School of Arts and Sciences, University of Pennsylvania, 231 South 34th Street, Philadelphia, Pennsylvania 19104, USA.*
[b] *Department of Biochemistry and Biophysics, Perelman School of Medicine, University of Pennsylvania, 421 Curie Boulevard, Philadelphia, PA 19104, USA.*
Supplementary Information available: Experimental methods, supplemental figures and tables, and associated references. See DOI: 10.1039/x0xx00000x

a thioamide quencher on the opposite of the scissile bond from the fluorophore; upon cleavage by proteolysis, these two will be separated, resulting in a turn-on of fluorescence that can be monitored in real time (**Fig. 1A**). We have systematically studied thioamide positional effects on our fluorescence sensor probes for cysteine proteases (papain, cathepsins L, V, K, B, and S) and serine proteases (trypsin, chymotrypsin, and kallikrein), identifying trends in perturbing and non-perturbing sites for thioamide labeling.[24] We have also tested thioamide peptides to determine whether they interfere with the cleavage of other substrates (showing that they bind at the active site).[21-23, 25] This initial screening allows us to use thioamide in one of three ways at a given site (**Fig. 1B**): 1) non-perturbing, interfering sites can be used for fluorescence protease sensors,[20] 2) perturbing, non-interfering sites can be used for *in vivo* therapeutic or imaging peptides (*e.g.,* thioamide-stabilized therapeutic GLP-1 or NPY-based cancer imaging probes),[21, 25] 3) perturbing, interfering sites can be used for selective protease inhibitors (*e.g.,* thioamide cathepsin L inhibitors).[23] Herein, we follow this workflow to develop thioamide peptide probes for DPP-4 based on its native substrates. Our probes, containing 7-methoxycoumarin-4-yl-alanine (Mcm or µ, **Fig. 2A**) as a fluorophore, can effectively report real-time DPP-4 activity in *in vitro* steady-state assays, inhibition assays, and saliva samples. We thus highlight the value of thioamides for the minimally perturbing design of substrate-based protease probes.

We based our first peptide probe design on NPY since it is known to be an excellent substrate of DPP-4.[4, 26] NPY is a natural 36-amino-acid neuromodulator that is abundant in the brain as well as in the peripheral nervous system.[27] NPY can modulate NPY receptors, which have been implicated in many diseases

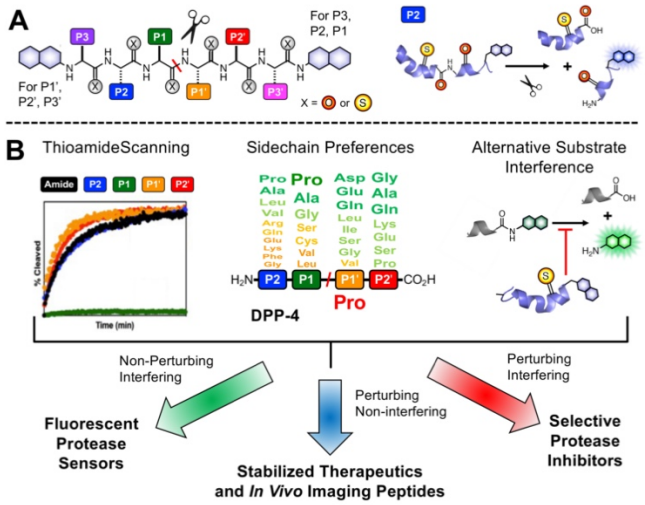


**Fig. 1.** Thioamide Applications in Protease Sensors, Peptide Stabilizers, and Inhibitors. (A) General design of thioamide protease sensor probes. Thioamides can quench a N- or C-terminally tagged fluorophore when they are in proximity; upon cleavage, there will be a turn on in fluorescent signal. Cleavage of a P2 thioamide peptide is shown as an example. (B) Information on thioamide effects on proteolysis rates from sensor probe assays, substrate sidechain preferences from literature studies and genetic data, and measurements of interference in cleavage of alternative substrates, can be leveraged for development of substrate-based thioamide probes. In this work, non-perturbing thioamide labeling can be used for the design of fluorescent protease sensors for DPP-4.

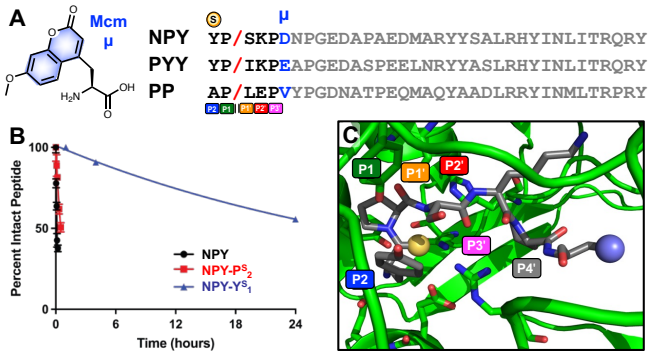


**Fig. 2.** Design of Substrate-based Thioamide Probes for DPP-4. (A) Sequences of DPP-4 substrates neuropeptide Y (NPY), peptide YY (PYY), and pancreatic polypeptide (PP), with N-terminal residues P2-P3' highlighted and the P4' position in blue, where the donor fluorophore Mcm (µ) is placed. (B) Cleavage by DPP-4 of full-length NPY, NPY-Y$^S_1$ (P2 thioamide), and NPY-P$^S_2$ (P1 thioamide) monitored by HPLC. (C) X-ray structure of DPP-4 (green) with a fragment of NPY bound (grey), showing the P2-P4' positions with the P2 thioamide shown as a yellow sphere and the Mcm sidechain shown as a blue sphere.

such as metabolic diseases, obesity, pain, cancer, and cardiovascular regulation. DPP-4 typically cleaves full-length NPY at $Pro_2$ at its N-terminus, resulting in $NPY_{3-36}$.[4, 5, 26] DPP-4 cleavage modulates NPY receptor selectivity since the $NPY_{3-36}$ fragment is no longer active toward the NPY Y1 receptor (with vasoconstrictive properties), yet has a strong affinity toward NPY Y2 and Y5 receptors (as a vascular growth ååfactor).[4, 5]

Since DPP-4 cleaves the NPY peptides at $Pro_2$, we have only two options for thioamide placement, at the first tyrosine residue $Y_1$ (P2 position) or at the second proline $P_2$ (P1 position). As a preliminary assessment, we synthesized the all-amide full-length NPY peptide, along with its P1 thioamide analog (NPY-P$^S_2$) and its P2 thioamide analog (NPY-Y$^S_1$), to evaluate which thioamide position on NPY would significantly perturb recognition by DPP-4. In these assays, cleavage of the peptides was monitored high-performance liquid chromatography (HPLC), and fragment identities were confirmed by matrix-assisted laser desorption ionization mass spectrometry (MALDI MS) (**Fig. 2B**, primary data are shown in ESI **Fig. S11-S13**). The P2 thioamide analog, NPY-P$^S_2$, cleaved 6.5 times slower than the all-amide counterpart, while the P1 thioamide, NPY-Y$^S_1$, cleaved 372 times slower. This is in contrast to our results with GLP-1 and GIP thioamidation, in which both P2 and P1 thioamides significantly retarded proteolysis.[25] Here, our data show that the P2 position is less perturbing for proteolysis, possibly because it is a proline residue, and that we should place the thioamide at the P2 position to create a quenching effect as desired while still being responsive to DPP-4 proteolysis.

For our probe design, we chose Mcm/µ as the fluorophore for the following reasons: (1) it is only slightly larger than Trp; (2) it is commercially available as Fmoc-µ-OH; (3) it can be easily incorporated into the peptide probes via solid phase peptide synthesis, and (4) it can be quenched by thioamides. Our lab also has previously successfully utilized Mcm-tagged peptides as proteolysis probes for different serine-, cysteine-, carboxyl-, and metallo-proteases.[20-22, 24] Since µ is quenched by thioamides via a PeT mechanism, they must be in close proximity.[19] Based on our results with NPY-P$^S_2$ and NPY-Y$^S_1$, as

 

well as an analysis of the crystal structure of DPP-4 with a fragment of NPY bound (PDB ID: 1r9n),[28] we decided to design a hexapeptide probe, with the thioamide at P2 position (*i.e.* the N terminus) and the fluorophore μ at the P4' position, since the DPP-4 active site is relatively open there while it makes close contacts with the P1' , P2', and P3' amino acids (**Fig. 2C**). P2 and P4' are 5 residues apart, predicted to give sufficient quenching based on our studies of thioamide PeT quenching.[19]

First, we synthesized probe analogs of NPY, with the sequence of YPSKPμ ($NPY_{1-5}$). For comparison, we synthesized both the all-amide and P2 thioamide version of this peptide, YP/SKPμ and $Y^{S}$P/SKPμ, where the / indicates the DPP-4 cleavage site (**Fig. 2A**). As a demonstration that we could study mutations at prime sites, we also made a probe based on the NPY mutation $Ser_3$-to-Leu ($NPY_{1-5}L_3$: YPLKPμ). The same design was applied to two other natural substrates from the pancreatic polypeptide family, where we synthesized and tested the hexapeptide probes based on the first 5 N-terminal amino acids of PYY ($PYY_{1-5}$: YPIKPμ) and PP ($PP_{1-5}$: APLEPμ). $NPY_{1-5}$ NMR data indicate that the probes are unstructured (ESI, **Fig. S25-S27**).

Each probe was incubated with DPP-4 and fluorescence intensity was monitored over time ($\lambda_{ex}$ = 325 nm; $\lambda_{em}$ = 390 nm). Significantly, our μ-labeled NPY P2 thioamide sensor, $Y^{s}$PSKPμ, was cleaved by DPP-4 with similar kinetics (**Fig. 3A**, $t_{1/2}$ = 26 min) to the full-length NPY P2 thioamide, NPY-$P^{S}_2$ ($t_{1/2}$ = 30 min). Interestingly, we observed a fluorescence turn-on even without a thioamide, which is presumably due to quenching by the N-terminal Tyr residue. In fact, for both NPY probes (**Fig. 3A** and **3B**) and the PYY probe (**Fig. 3C**), we observed the synergic effects of both Tyr and thioamide quenching. In the case of the PP-based probe, since there was no tyrosine, the thiopeptide showed its full utility as the all-amide APLEPμ had no fluorescence quenching, while the thioamide version $A^{S}$PLEPμ showed good fluorescence turn-on (**Fig. 3D**). To ensure that the fluorescence assays truly reflect protease cleavage, HPLC and MALDI were used to confirm cleavage product identities (ESI, **Fig. S14-S17**; **Tables S4-S7**). The P1' mutated $NPY_{1-5}L_3$ probe, $Y^{S}$PLKPμ, is cleaved 2-fold slower than the native $NPY_{1-5}$ probe, $Y^{S}$PSKPμ, and $PYY_{1-5}$, which also differs at the P1' site ($Y^{S}$PIKPμ), is cleaved 3-fold slower than $NPY_{1-5}$. These data demonstrate that we can create probes to explore the effects of mutations on the prime sites of a substrate, which could not be achieved with commercially available probes such as GP-AMC.

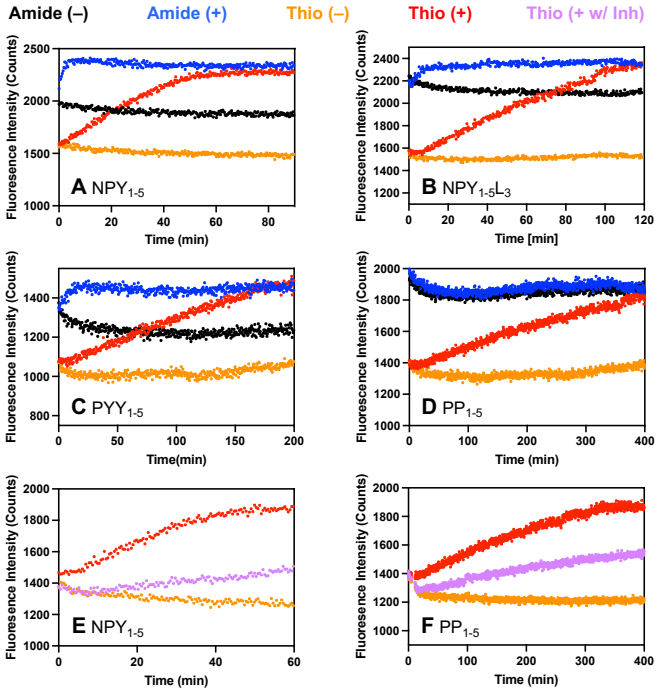


**Fig. 3.** DPP-4 Proteolysis Probes based on Native Substrates from the Pancreatic Polypeptide Family. (A-F) Fluorescence turn-on occurs upon DPP-4 cleavage due to relief of thioamide quenching and/or Tyr quenching. The (-) indicates the absence of protease and the (+) indicates the presence of protease. For thioamide $NPY_{1-5}$ and $PP_{1-5}$ peptides, (E-F) assays were also done with the protease and 50 nM inhibitor sitagliptin (+ w/ Inh). The fluorescence was monitored as a function of time at 390 nm with excitation at 325 nm on a Tecan Spark plate reader. All traces show the average of three replicates.

To ensure that our probes are responsive to the presence of inhibitors, inhibition studies were done with 50 nM sitagliptin, which is a selective inhibitor of DPP-4 with an $IC_{50}$ between 18-87 nM, depending on the experiment.[10, 29] In all cases, we observed inhibition by sitagliptin with our probes, as indicated by a decrease in fluorescence signal in the presence of 50 nM sitagliptin consistent with ~50% inhibition (NPY and PP probe data shown in **Fig. 3E**/**3F**; NPY-$L_3$ and YY probe data show in ESI **Fig. S19**). At higher concentrations of sitagliptin, we observe complete inhibition (ESI **Fig. S20**). This shows the potential of using our probes in inhibitor screening in biochemical assays, which is an important application for drug development and mechanistic studies.

We also wished to demonstrate that our probes could be used as a tool to quickly detect DPP-4 activity in biological samples. For instance, DPP-4 activity in saliva has been associated with diseases such as periodontitis and the presence of *Porphyromonas gingivalis*, Sjögren's syndrome, and oral cancers.[30-32] Herein, following a very simple protocol, we directly added our thioamide probes to human saliva, then measured fluorescence changes with a plate reader (**Fig. 4A**). For our NPY- and PYY-based probes, we observed an increase in fluorescence in the presence of saliva in the first two hours of incubation ($NPY_{1-5}$ probe data shown in **Fig. 4B**, $NPY_{1-5}L_3$ and $PYY_{1-5}$ probe data shown in ESI **Fig. S22**). For $PP_{1-5}$, a slower increase in fluorescence was observed (**Fig. 4C**), consistent with slower rates in the DPP-4 only assay. The fluorescence increases could be completely blocked by sitagliptin, showing that they are highly specific for DPP-4 (**Fig. 4** and ESI **Fig. S23**). To approximate saliva samples from cancer patients, where DPP-4 activity levels are 2-4 fold higher than in controls, we added DPP-4 to the saliva and found that we could easily detect these differences (**Fig. 4B/C**). These results show the potential for our probes to measure DPP-4 in biological samples.

Here, we have demonstrated that we can create thioamide probes to detect DPP-4 activity using substrate-based probes that not only include the dipeptide recognition motif, but also native sequences on the primed side of the scissile bond – something that is not featured in many of the existing probes. This close mimicking of the native substrate allows our probes to report DPP-4 activity as faithfully as possible. Given the promising results from the human saliva assays, we will further

test with actual patient samples. We will take advantage of the thioamide's ability to quench other fluorophores[19] to make cellular or in vivo imaging probes with red-shifted dyes, as in many recent cancer imaging probes.[33, 34]

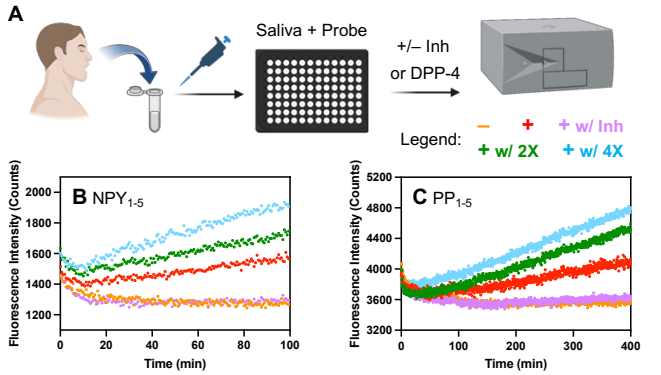


**Figure 4.** DPP-4 Detection in Human Saliva. (A) Assay workflow, created with Biorender.com. (B,C) For each assay, 25 µL of human saliva (+), saliva with 250 ng/L (+ w/ 2X) or 500 ng/L (+ w/ 4X) additional DPP-4, PBS (-), or saliva with 500 nM sitagliptin (+ w/ Inh) was added to 25 µL of 5 µM $NPY_{1-5}$ or 15 µM $PP_{1-5}$ thioamide probe. The fluorescence was monitored as a function of time at 390 nm with excitation at 325 nm on a Tecan Spark plate reader. Traces show the average of three replicates.

## Author contributions and acknowledgements

The manuscript was written by H.A.T.P. and E.J.P., with input from all authors. H.A.T.P. designed all experiments and H.A.T.P. and Y.C. performed most experiments. S.A.E. synthesized full-length NPY constructs. This research was supported by a grant from the National Science Foundation to E.J.P. (NSF CHE-2203909). The MALDI MS was acquired through a National Institutes of Health instrumentation grant (NIH S10-OD030460).

## Data availability

The data supporting this article have been included as part of the Supplementary Information.

## Notes and references

1 C. F. Deacon, *Front Endocrinol (Lausanne)*, 2019, **10**, 80.
2 W. Jungraithmayr and N. Enz, *Cell Mol Immunol*, 2020, **17**, 1208-1209.
3 V. K. Hopsu-Havu and G. G. Glenner, *Histochemie*, 1966, **7**, 197-201.
4 A. M. Lambeir, C. Durinx, S. Scharpe and I. De Meester, *Crit Rev Clin Lab Sci*, 2003, **40**, 209-294.
5 E. E. Mulvihill and D. J. Drucker, *Endocr Rev*, 2014, **35**, 992-1019.
6 N. M. Sherwood, S. L. Krueckl and J. E. McRory, *Endocrine Reviews*, 2000, **21**, 619-670.
7 J. J. Holst, C. Orskov, O. V. Nielsen and T. W. Schwartz, *FEBS Lett*, 1987, **211**, 169-174.
8 W. Kim and J. M. Egan, *Pharmacol Rev*, 2008, **60**, 470-512.
9 B. Manandhar and J. M. Ahn, *J Med Chem*, 2015, **58**, 1020-1037.
10 D. Kim, L. Wang, M. Beconi, G. J. Eiermann, M. H. Fisher, H. He, G. J. Hickey, J. E. Kowalchick, B. Leiting, K. Lyons, F. Marsilio, M. E. McCann, R. A. Patel, A. Petrov, G. Scapin, S. B. Patel, R. S. Roy, J. K. Wu, M. J. Wyvratt, B. B. Zhang, L. Zhu, N. A. Thornberry and A. E. Weber, *J Med Chem*, 2005, **48**, 141-151.
11 A. L. Sun, J. T. Deng, G. J. Guan, S. H. Chen, Y. T. Liu, J. Cheng, Z. W. Li, X. H. Zhuang, F. D. Sun and H. P. Deng, *Diab Vasc Dis Res*, 2012, **9**, 301-308.
12 O. J. Cordero, R. Varela-Calvino, T. Lopez-Gonzalez, C. Calvino-Sampedro, J. E. Vinuela, C. Mourino, I. Hernandez-Rodriguez, M. Rodriguez-Lopez, B. Aspe de la Iglesia and J. M. Pego-Reigosa, *PLoS One*, 2015, **10**, e0131992.
13 G. Firneisz, T. Varga, G. Lengyel, J. Feher, D. Ghyczy, B. Wichmann, L. Selmeci, Z. Tulassay, K. Racz and A. Somogyi, *PLoS One*, 2010, **5**, e12226.
14 X. Guo, S. Mu, J. Li, Y. Zhang, X. Liu, H. Zhang and H. Gao, *J Mater Chem B*, 2020, **8**, 767-775.
15 A. Ogasawara, M. Kamiya, K. Sakamoto, Y. Kuriki, K. Fujita, T. Komatsu, T. Ueno, K. Hanaoka, H. Onoyama, H. Abe, Y. Tsuji, M. Fujishiro, K. Koike, M. Fukayama, Y. Seto and Y. Urano, *Bioconj Chem*, 2019, **30**, 1055-1060.
16 N. H. Ho, R. Weissleder and C. H. Tung, *Bioorg Med Chem Lett*, 2006, **16**, 2599-2602.
17 L.-W. Zou, P. Wang, X.-K. Qian, L. Feng, Y. Yu, D.-D. Wang, Q. Jin, J. Hou, Z.-H. Liu, G.-B. Ge and L. Yang, *Biosensors and Bioelectronics*, 2017, **90**, 283-289.
18 K. Kuhn-Wache, J. W. Bar, T. Hoffmann, R. Wolf, J. U. Rahfeld and H. U. Demuth, *Biol Chem*, 2011, **392**, 223-231.
19 J. M. Goldberg, S. Batjargal, B. S. Chen and E. J. Petersson, *J Am Chem Soc*, 2013, **135**, 18651-18658.
20 J. M. Goldberg, X. Chen, N. Meinhardt, D. C. Greenbaum and E. J. Petersson, *J Am Chem Soc*, 2014, **136**, 2086-2093.
21 T. M. Barrett, X. S. Chen, C. Liu, S. Giannakoulias, H. A. T. Phan, J. Wang, E. K. Keenan, R. J. Karpowicz, Jr. and E. J. Petersson, *ACS Chem Biol*, 2020, **15**, 774-779.
22 C. Liu, T. M. Barrett, X. Chen, J. J. Ferrie and E. J. Petersson, *ChemBioChem*, 2019, **20**, 2059-2062.
23 H. A. T. Phan, S. G. Giannakoulias, T. M. Barrett, C. Liu and E. J. Petersson, *Chem Sci*, 2021, **12**, 10825-10835.
24 S. Giannakoulias, S. R. Shringari, C. Liu, H. A. T. Phan, T. M. Barrett, J. J. Ferrie and E. J. Petersson, *J Phys Chem B*, 2020, **124**, 8032-8041.
25 X. Chen, E. G. Mietlicki-Baase, T. M. Barrett, L. E. McGrath, K. Koch-Laskowski, J. J. Ferrie, M. R. Hayes and E. J. Petersson, *J Am Chem Soc*, 2017, **139**, 16688-16695.
26 R. Mentlein, P. Dahms, D. Grandt and R. Krüger, *Regul Pept*, 1993, **49**, 133-144.
27 S. P. Brothers and C. Wahlestedt, *EMBO Mol Med*, 2010, **2**, 429-439-439.
28 K. Aertgeerts, S. Ye, M. G. Tennant, M. L. Kraus, J. Rogers, B.-C. Sang, R. J. Skene, D. R. Webb and G. S. Prasad, *Protein Sci*, 2004, **13**, 412-421.
29 J. Zhang, X. K. Qian, P. F. Song, X. D. Li, A. Q. Wang, H. Huo, J. C. Yao, G. M. Zhang and L. W. Zou, *Anal Methods*, 2021, **13**, 2671-2678.
30 K. Fukasawa, M. Harada, M. Komatsu, M. Yamaoka, M. Urade, K. Shirasuna and T. Miyazaki, *Int J Oral Surgery*, 1982, **11**, 246-250.
31 P. Aemaimanan, N. Sattayasai, N. Wara-aswapati, W. Pitiphat, W. Suwannarong, S. Prajaneh and S. Taweechaisupapong, *J Periodontol*, 2009, **80**, 1809-1814.
32 L. Garreto, S. Charneau, S. C. Mandacaru, O. T. Nobrega, F. N. Motta, C. N. de Araujo, A. C. Tonet, F. M. B. Modesto, L. M. Paula, M. V. de Sousa, J. M. Santana, A. C. Acevedo and I. M. D. Bastos, *Front Immunol*, 2021, **12**, 686480.
33 R. Sun, W. Ma, M. Ling, C. Tang, M. Zhong, J. Dai, M. Zhu, X. Cai, G. Li, Q. Xu, L. Tang, Z. Yu and Z. Peng, *J Control Release*, 2022, **350**, 525-537.
34 M. Tian, R. Wu, C. Xiang, G. Niu and W. Guan, *Moleculesl*, 2024, **29**, 1420-3049.

 

# *Thioamide-based Fluorescent Sensors for Dipeptidyl Peptidase 4*

Hoang Anh T. Phan,[a] Yanan Chang,[a] Samuel A. Eaton,[a] E. James Petersson [a]

[a] *Department of Chemistry, University of Pennsylvania, Philadelphia, Pennsylvania 19104, USA*

[*]Email: ejpetersson@sas.upenn.edu

## Table of Contents

1. General Information ..... 2
2. Peptide Synthesis, Purification, and Characterization ..... 3
3. DPP-4 Proteolysis Assays with Full-Length NPY Peptides (HPLC) ..... 17
4. DPP-4 Proteolysis Assays (Steady State Assays) ..... 21
5. Sitagliptin Inhibition of DPP-4 ..... 26
6. Human Saliva Assays ..... 29
7. DPP-4 Inhibition with Sitagliptin in Human Saliva ..... 31
8. Human Saliva Doped with Additional DPP-4 ..... 33
9. Nuclear Magnetic Resonance (NMR) ..... 34
10. References ..... 36

## 1. General Information

Fluorenylmethoxycarbonyl-β-(7-methoxycoumarin-4-yl)-Ala-OH were purchased from Bachem (Torrance, CA, USA). All other fluorenylmethoxycarbonyl (Fmoc) protected amino acids were purchased from Novabiochem (currently EMD Millipore, MilliporeSigma; Burlington, MA, USA). (7-Azabenzotriazol-1-yloxy)tripyrrolidino-phosphonium hexafluorophosphate (PyAOP) was purchased from Chem-Impex (Wood Dale, IL, USA). Piperidine, *N*,*N*-diisopropylethylamine (DIPEA), dipeptidyl Peptidase IV human (DPP-4, recombinant, expressed in Sf9 cells), and sitagliptin (DPP-4 specific inhibitor, ≥98% by HPLC; SML3205) were purchased from Sigma-Aldrich (St. Louis, MO, USA). Fluorescent H-Gly-Pro-AMC (DPP-4 substrate, lyophilized, ≥95% by HPLC) was purchased from AnaSpec. Pooled human saliva (IRHUSL5ML) was purchased from Innovative Research (Novi, MI, USA). All other reagents were purchased from Fisher Scientific (Pittsburgh, PA, USA) unless specified otherwise. Milli-Q filtered (18 MΩ) water was used for all solutions (EMD Millipore). Peptides were purified with an Agilent 1260 Infinity II Preparative HPLC system and analyzed with an Agilent 1260 Infinity II Analytical HPLC system (Santa Clara, CA, USA). Peptide mass spectrometry was collected with a Bruker Ultraflex III matrix-assisted laser desorption ionization mass spectrometer (MALDI MS), Bruker MicrofleX (MALDI-TOF MS), or Bruker RapifleX (MALDI-TOF/TOF) (Billerica, MA, USA). Time-course UV-Vis absorbance and fluorescence data were obtained with a Tecan Infinite® M1000 PRO plate reader (Männedorf, Switzerland). The NMR spectra was collected with AVANCE NEO 600 MHz NMR.

## 2. Peptide Synthesis, Purification, and Characterization

**Synthesis of Thioamino acid Precursors.** $N_\alpha$-Fmoc-L-thiotyrosine(tBu)-nitrobenzotriazolide, $N_\alpha$-Fmoc-L-thioproline-nitrobenzotriazolide, and $N_\alpha$-Fmoc-L-thioalanine-nitrobenzotriazolide were synthesized and characterized using previously published procedures by our laboratory.[1, 2]

**Peptide Synthesis of Full-length $NPY_{1-36}$ Peptides.** $NPY_{1-36}$ was purchased from Genscript. Fmoc-protected $NPY_{3-36}$ (Fmoc-SKPDNPGEDAPAEDMARYYSALRHYINLITRQRY; molecular weight = 4233.66 g/mol) was purchased on resin from GenScript. Each peptide was manually synthesized on a 10 μmol scale. The resin was initially added to a dry reaction vessel (RV) and swelled in 2 mL dimethylformamide (DMF) for 30 min with magnetic stirring. After washing and swelling, the resin was incubated with 1 mL of 20% piperidine solution in DMF for 20 mins under stirring for deprotection. The same deprotection procedure was followed for all the subsequent standard amino acids. Between each reaction, the resin was washed extensively with adequate DMF, DCM, and DMF. For a typical 45-minute coupling reaction, 5 equiv. of the standard amino acid and 5 equiv. of PyAOP was dissolved in 1 mL DMF, and added to the RV, with an addition of 10 equiv. of DIPEA. Thioamides were coupled using a modified procedure: for the P1 thioamide peptide ($NPY_{1-36}$-$P^S_2$) and P2 thioamide analog ($NPY_{1-36}$-$Y^S_1$), 3 equiv. of the thioamide precursor was dissolved in 1 mL of dry dichloromethane (DCM) with 6 equiv. DIPEA and stirred for 30 minutes. This procedure was repeated prior to deprotection to ensure efficient incorporation of the thioaminoacid onto the peptide chains. For the deprotection of thioamides, 1 mL of 2% DBU (1,8-diazabicyclo(5.4.0)undec-7-ene) in DMF was added to the RV and reacted three times for 2 min each, with extensive washing with DMF and DCM between each deprotection step.

**Peptide Synthesis of Short NPY-based Fluorescent Probes.** Each peptide was manually synthesized on a 25 or 100 μmol scale on 2-chlorotrityl resin based on our established protocols.[3] For a typical synthesis, 2-chlorotrityl resin was added to a dry RV and initially swelled in 5 mL DMF for 30 min with magnetic stirring. Between each reaction, the resin was washed extensively with adequate DMF, DCM, and DMF. If the first amino acid was Fmoc-β-(7-methoxycoumarin-4-yl)-Ala-OH, 2 equiv. of the amino acid was dissolved in 1 mL of DMF with 4 equiv. of DIPEA and stirred for 30 min; this reaction was repeated to ensure efficient coupling. A methanol capping step with 5% methanol in DMF could be done after the first amino acid coupling to ensure that there was no reactive resin. After washing, the resin was incubated with 2 mL of 20% piperidine solution in DMF for 20 mins under stirring for deprotection. The same deprotection procedure was followed for all the subsequent standard amino acids. For a typical 45-minute coupling reaction, 5 equiv. of the standard amino acid and 5 equiv. of PyAOP was dissolved in 1 mL DMF, and added to the RV, with an addition of 10 equiv. of DIPEA. Thioamide residues were coupled and deprotected with slightly modified procedures. Thioamides were coupled through pre-activated precursors, where 3 equiv. of the thioamide precursor was dissolved in 1.5 mL of dry dichloromethane (DCM) with 5 equiv. DIPEA and stirred for 45 minutes. This procedure was repeated prior to deprotection to ensure efficient incorporation of the thioaminoacid onto the peptide chains. For the deprotection of thioamides, 2 mL of 2% DBU (1,8-diazabicyclo(5.4.0)undec-7-ene) in DMF was added to the RV and reacted three times for 2 min each, with extensive washing with DMF and DCM between each deprotection step.

**Peptide Cleavage and Purification.** Upon completion of the synthesis, the resin was dried with DCM under vacuum. Peptides were cleaved from resin by treatment with a 1-2 mL fresh cleavage cocktail of trifluoroacetic acid (TFA), water, and triisopropylsilane (TIPSH) (95:2.5:2.5 v/v) for 45 mins with stirring. After treatment, the cocktail solution was expelled from the RV with nitrogen and reduced to a volume of less than 1 mL by rotary evaporation. This resulting solution was then treated with over 10 mL of cold ethyl ether to precipitate out the peptides. This precipitate was flash frozen with liquid nitrogen and evaporated using lyophilization. The crude peptide was diluted in $CH_3CN/H_2O$ (10:90 v/v) and then purified on a Luna® Omega 5 µm PS C18 100 Å, LC semi-preparative column (Phenomenex; Torrance, CA, USA) by HPLC using the following gradients at a flow rate of 3 mL/min; the full-length peptide was purified using a C4 column (**Table S1** and **Table S2**). The HPLC chromatograms of the first-pass purification are shown in **Figures S1– S10**. MALDI MS was used to confirm peptide identities; the identified masses summarized in **Table S3** and the MALDI MS spectra are shown in **Figures S1-S10**. Purified peptides were dried on a lyophilizer (Labconco; Kansas City, MO, USA) or in a vacuum centrifuge (Savant/Thermo Scientific; Rockford, IL, USA). If necessary, peptides were subjected to multiple rounds of purification until 99% purity by analytical HPLC was achieved.

**Table S1**. Peptide Purification Methods and Retention Time.

| Peptide | Gradient | Retention Time |
|---|---|---|
| $NPY_{1-36}$-$Y^S_1$ | 1 | 25.3 min |
| $NPY_{1-36}$-$P^S_2$ | 1 | 25.4 min |
| YPSKPμ | 2 | 17.4 min |
| $Y^S$PSKPμ | 2 | 17.1 min |
| YPLKPμ | 3 | 15.6 min |
| $Y^S$PLKP-μ | 3 | 18.7 min |
| YPIKPμ | 3 | 16.0 min |
| $Y^S$PIKP-μ | 3 | 16.5 min |
| APLEP-μ | 3 | 19.2 min |
| $A^S$PLEP-μ | 3 | 19.5 min |

* Abbreviations: μ: 7-methoxycoumarinylalanine; $Y^S$: thiotyrosine; $P^S$: thioproline; $A^S$: thioalanine.

**Table S2**. HPLC Gradients for Peptide Purification.

| No. | Time (min) | % B | No. | Time (min) | % B |
|---|---|---|---|---|---|
| 1 | 0:00 | 10 | 2 | 0:00 | 10 |
| | 2:00 | 20 | | 3:00 | 10 |
| | 5:00 | 20 | | 5:00 | 10 |
| | 35:00 | 50 | | 25:00 | 30 |
| | 36:00 | 50 | | 27:00 | 100 |
| | 37:00 | 100 | | 30:00 | 100 |
| | 39:00 | 100 | | 34:00 | 10 |
| | 43:00 | 10 | | 35:00 | 10 |
| | 45:00 | 10 | | | |
| 3 | 0:00 | 10 | | | |
| | 3:00 | 20 | | | |
| | 5:00 | 20 | | | |
| | 25:00 | 40 | | | |
| | 27:00 | 100 | | | |
| | 30:00 | 100 | | | |
| | 34:00 | 10 | | | |
| | 35:00 | 10 | | | |

* Solvent A: 0.1 % TFA in water; Solvent B: 0.1 % TFA in acetonitrile

**Table S3**. Calculated and Observed Masses of Peptides.

| Peptide | $[M+H]^+$ | | $[M+Na]^+$ | | $[M+K]^+$ | |
|---|---|---|---|---|---|---|
| | Calculated | Observed | Calculated | Observed | Calculated | Observed |
| $NPY_{1-36}$-$Y^S_1$ | 4287.05 | 4287.145 | 4309.03 | - | 4325.00 | - |
| $NPY_{1-36}$-$P^S_2$ | 4287.05 | 4287.729 | 4309.03 | - | 4325.00 | - |
| YPSKPμ | 836.39 | 836.054 | 858.37 | 858.067 | 874.34 | 874.035 |
| $Y^S$PSKPμ | 852.36 | 852.017 | 874.24 | 874.010 | 890.31 | 890.606 |
| YPLKPμ | 863.00 | 862.471 | 884.98 | 884.457 | 901.09 | 900.432 |
| $Y^S$PLKPμ | 879.06 | 878.449 | 901.04 | 900.429 | 917.15 | 916.404 |
| YPIKPμ | 862.44 | 862.626 | 884.320 | 884.605 | 900.39 | 900.172 |
| $Y^S$PIKPμ | 878.41 | 878.140 | 900.39 | 900.118 | 916.37 | 916.084 |
| APLEPμ | 771.85 | 771.415 | 793.83 | 793.398 | 809.94 | 809.371 |
| $A^S$PLEPμ | 787.91 | 787.394 | 809.89 | 809.378 | 826.00 | 825.382 |

* Abbreviations: μ: 7-methoxycoumarinylalanine; $Y^S$: thiotyrosine; $P^S$: thioproline; $A^S$: thioalanine

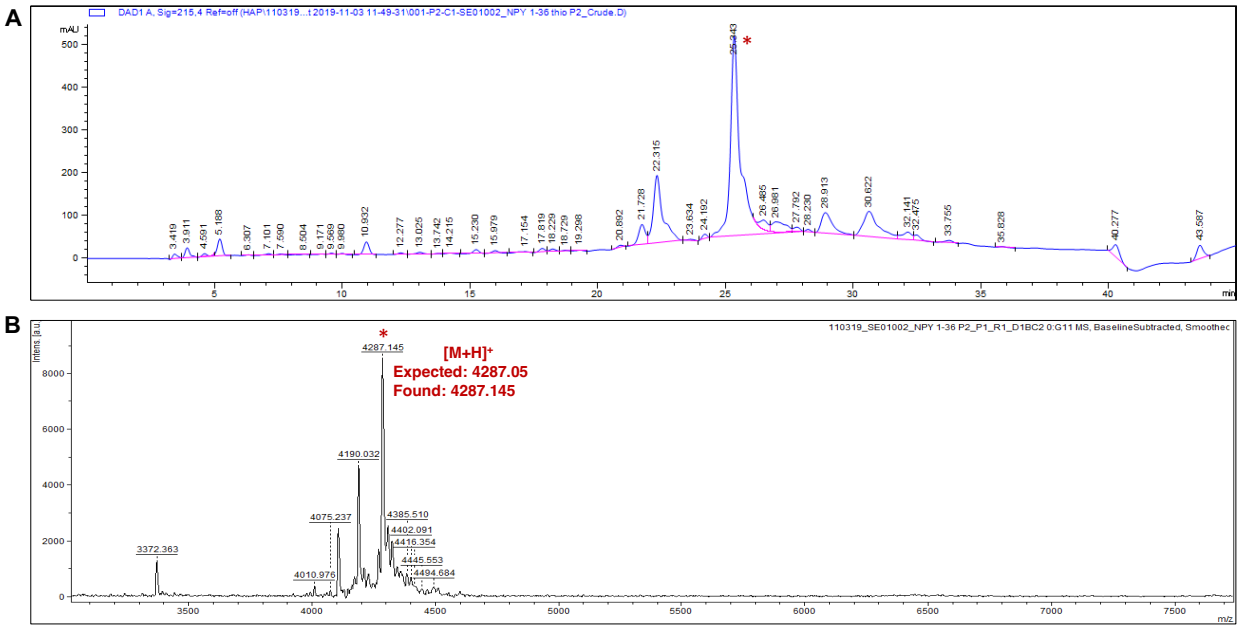


**Figure S1.** Purification and Characterization of $NPY_{1\text{-}36}\text{-}Y^{S}{}_{1}$ Peptide. (A) HPLC chromatogram of crude peptide sample. (B) MALDI-TOF MS spectrum of the peptide. The stars indicate the peak for the peptide product and its identified mass.

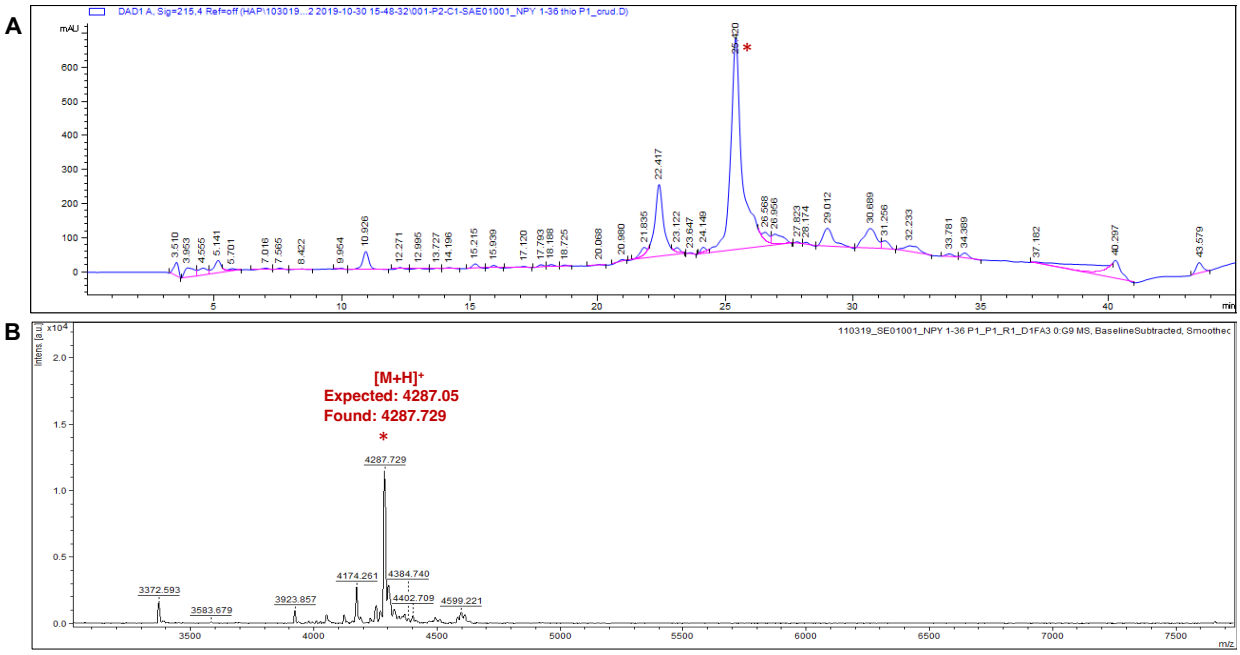


**Figure S2.** Purification and Characterization of $NPY_{1\text{-}36}\text{-}P^{S}{}_{2}$ Peptide. (A) HPLC chromatogram of crude peptide sample. (B) MALDI-TOF MS spectrum of the peptide. The stars indicate the peak for the peptide product and its identified mass.

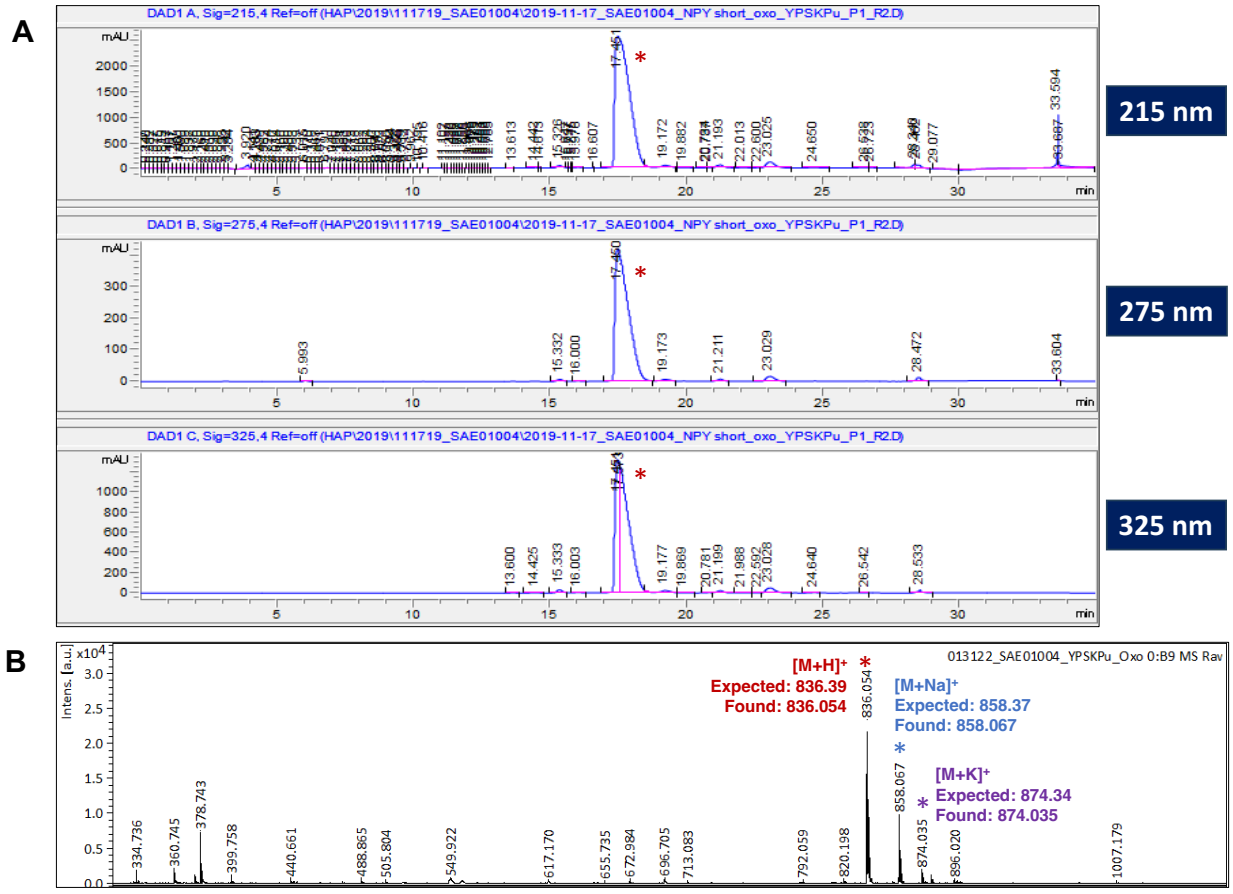


**Figure S3.** Purification and Characterization of YPSKPμ Peptide. (A) HPLC chromatogram of crude peptide sample; different wavelengths were monitored - 215 nm, 275 nm, and 325 nm. (B) MALDI-TOF MS spectrum of the peptide. The stars indicate the peak for the peptide product and its identified masses.

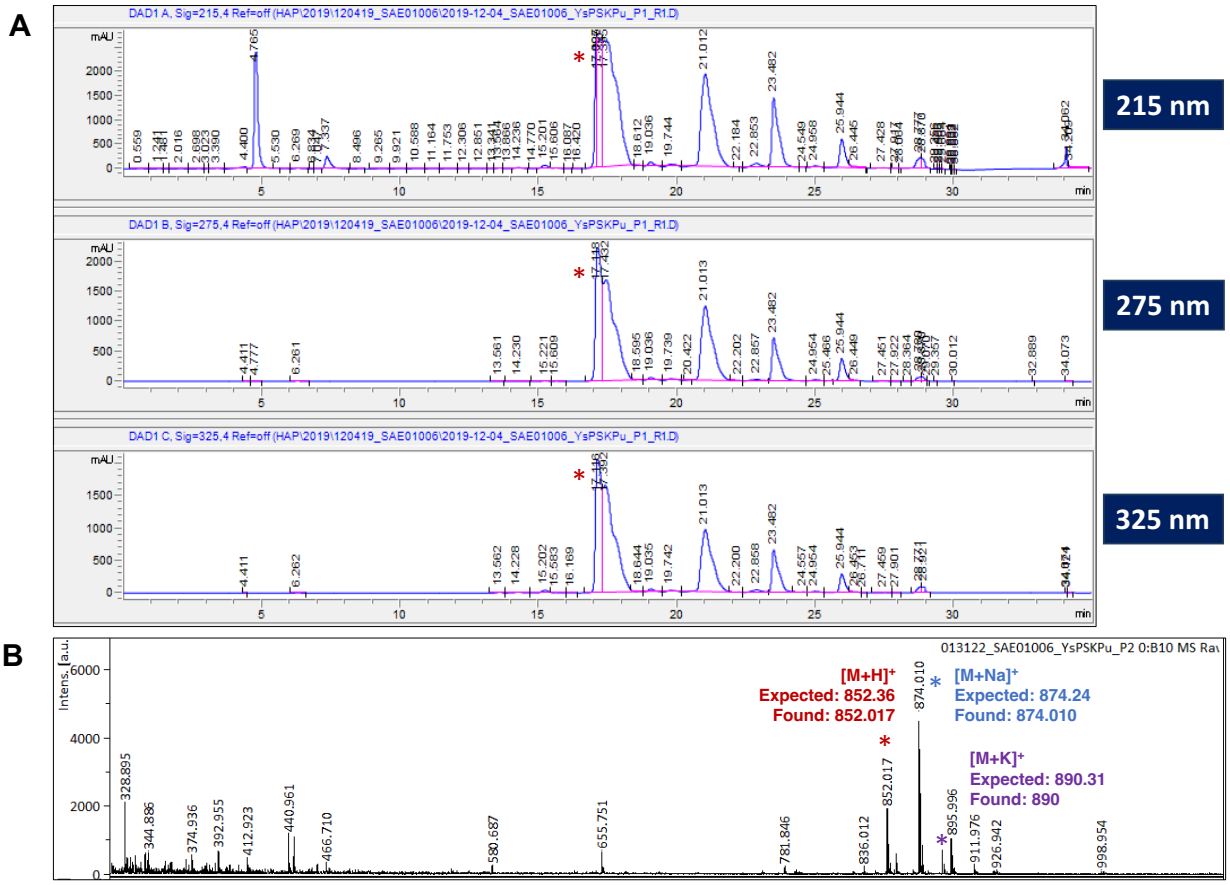


**Figure S4.** Purification and Characterization of Y$^{S}$PSKPμ Peptide. (A) HPLC chromatogram of crude peptide sample; different wavelengths were monitored - 215 nm, 275 nm, and 325 nm. (B) MALDI-TOF MS spectrum of the peptide. The stars indicate the peak for the peptide product and its identified masses.

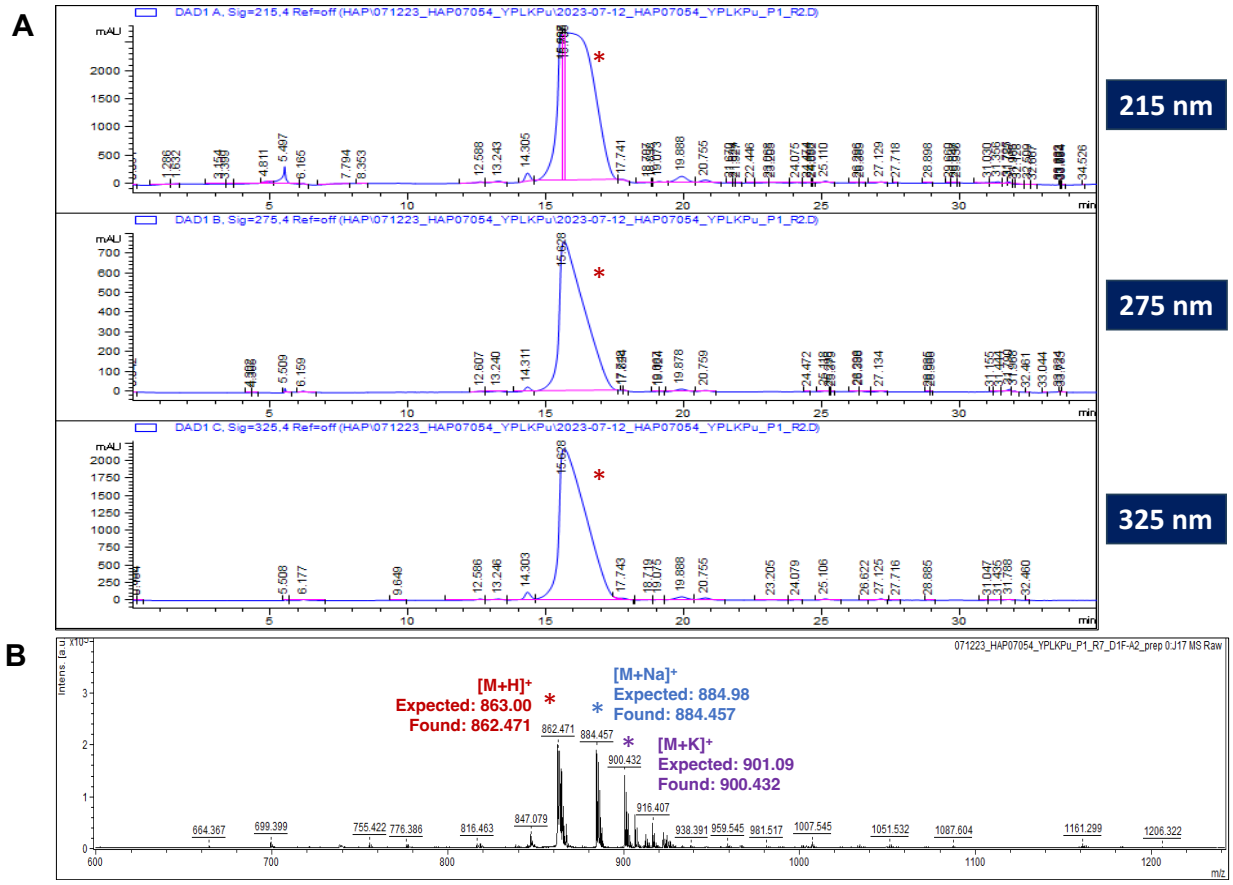


**Figure S5.** Purification and Characterization of YPLKPμ Peptide. (A) HPLC chromatogram of crude peptide sample; different wavelengths were monitored - 215 nm, 275 nm, and 325 nm. (B) MALDI-TOF MS spectrum of the peptide. The stars indicate the peak for the peptide product and its identified masses.

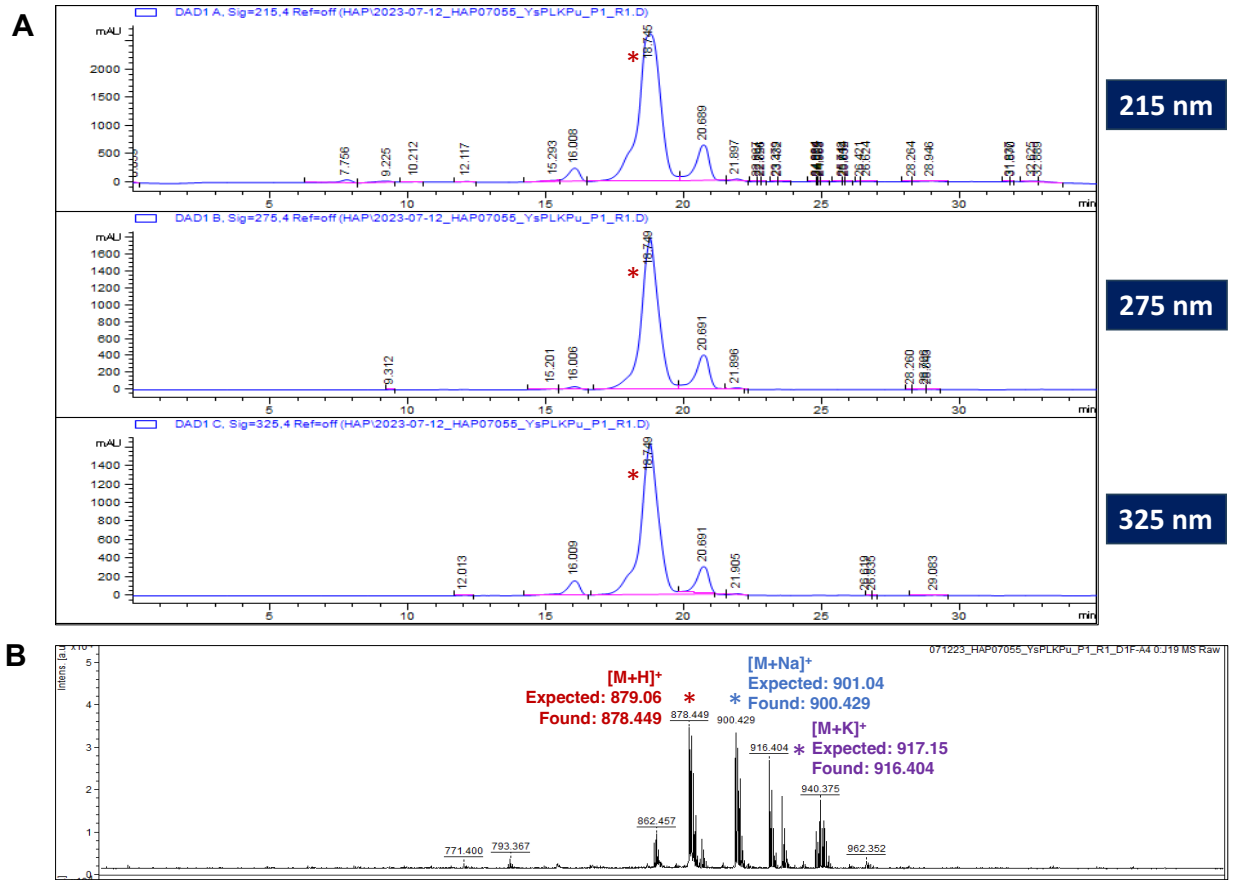


**Figure S6.** Purification and Characterization of Y$^{S}$PLKPμ Peptide. (A) HPLC chromatogram of crude peptide sample; different wavelengths were monitored - 215 nm, 275 nm, and 325 nm. (B) MALDI-TOF MS spectrum of the peptide. The stars indicate the peak for the peptide product and its identified masses.

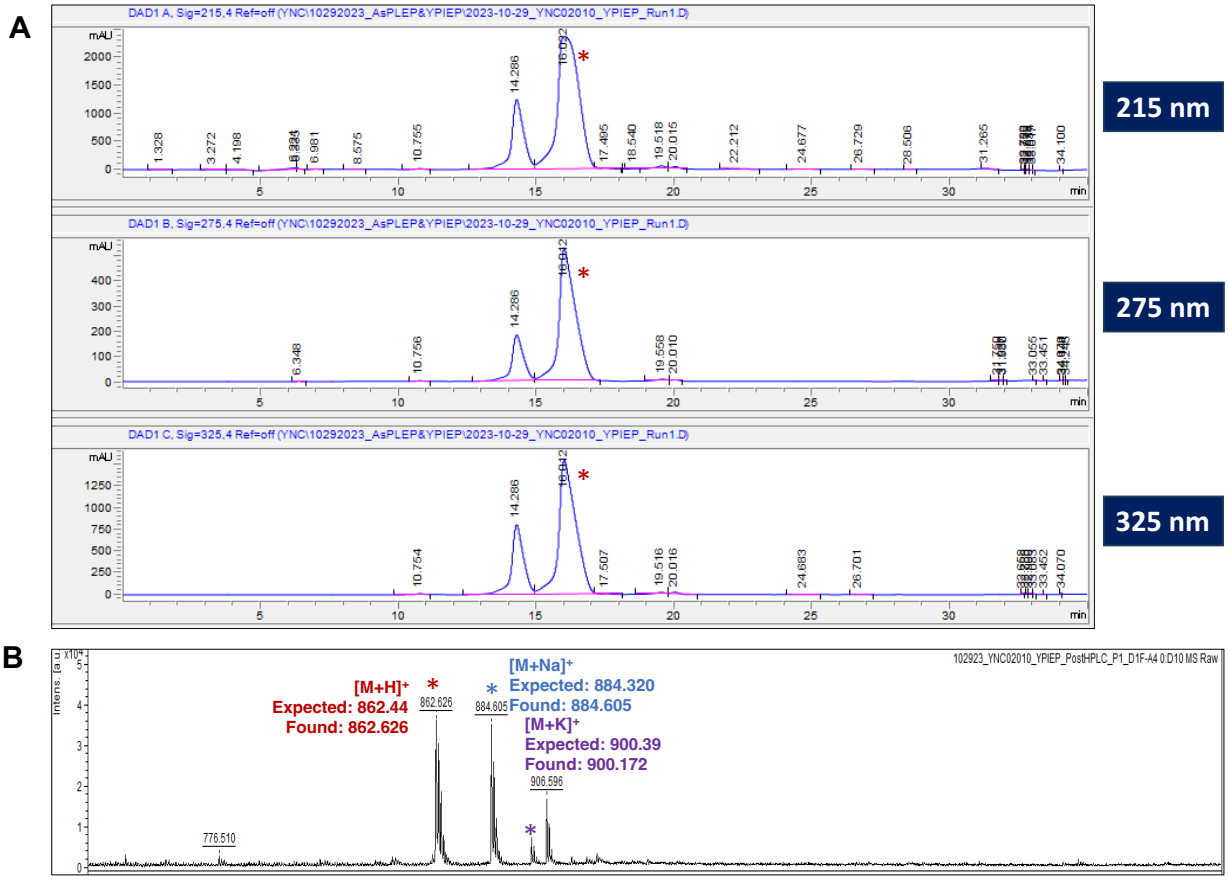


**Figure S7.** Purification and Characterization of YPIKPμ Peptide. (A) HPLC chromatogram of crude peptide sample; different wavelengths were monitored - 215 nm, 275 nm, and 325 nm. (B) MALDI-TOF MS spectrum of the peptide. The stars indicate the peak for the peptide product and its identified masses.

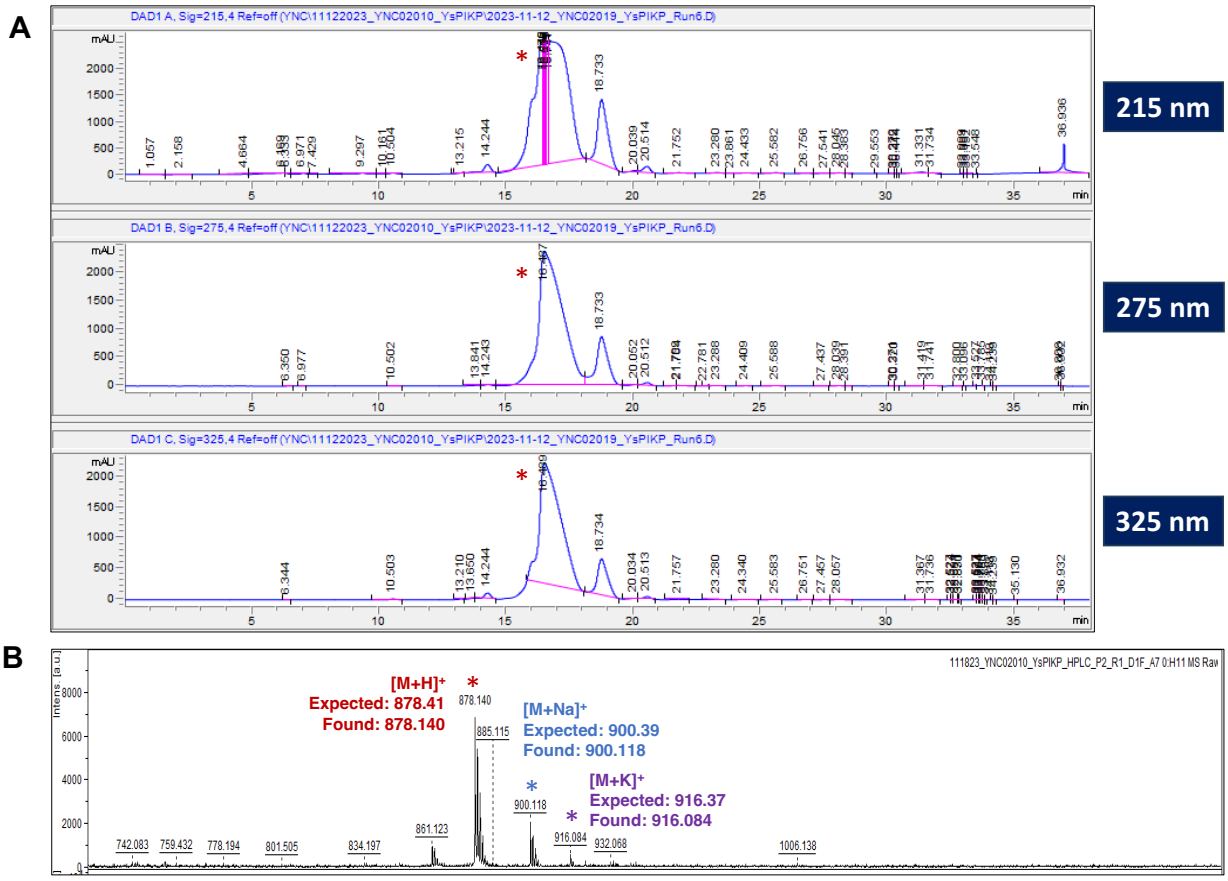


**Figure S8.** Purification and Characterization of Y$^{S}$PIKPμ Peptide. (A) HPLC chromatogram of crude peptide sample; different wavelengths were monitored - 215 nm, 275 nm, and 325 nm. (B) MALDI-TOF MS spectrum of the peptide. The stars indicate the peak for the peptide product and its identified masses.

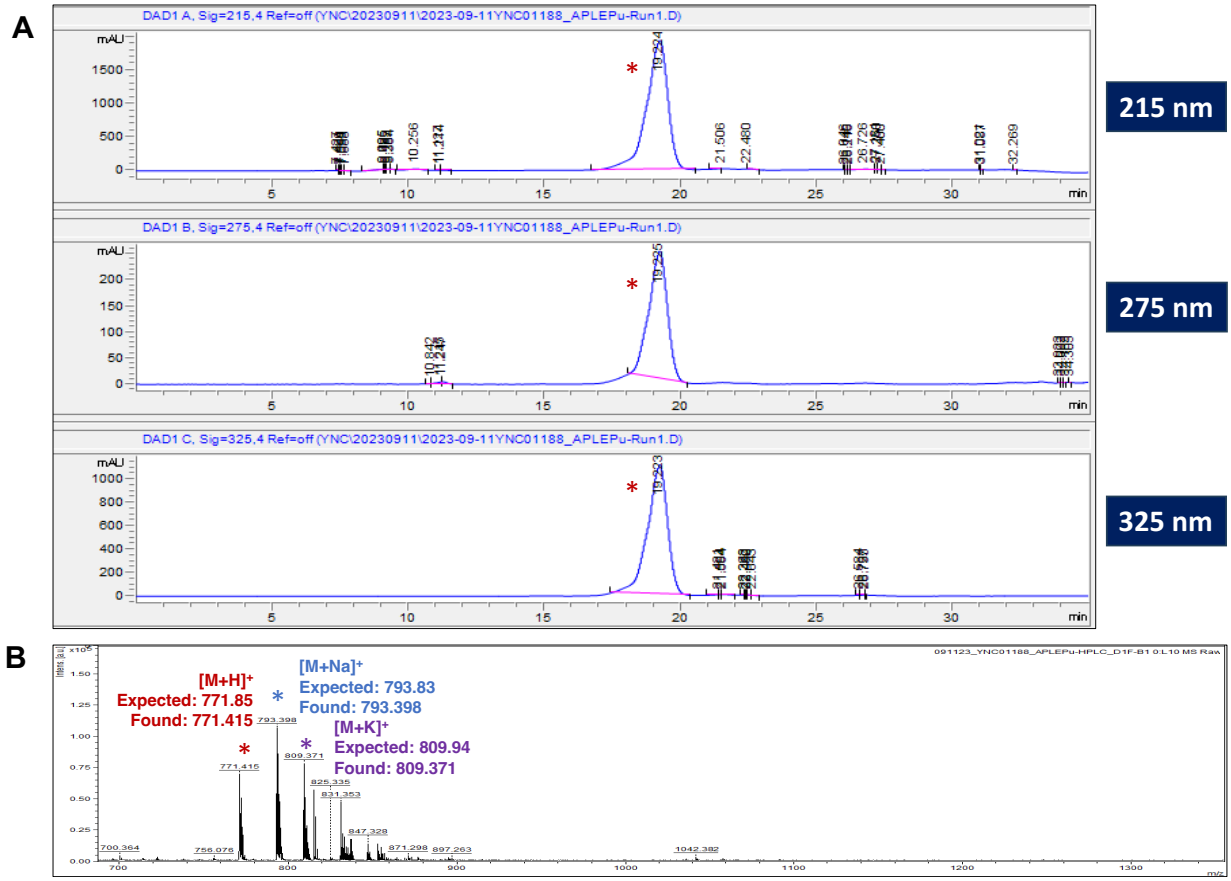


**Figure S9.** Purification and Characterization of APLEPμ Peptide. (A) HPLC chromatogram of crude peptide sample; different wavelengths were monitored - 215 nm, 275 nm, and 325 nm. (B) MALDI-TOF MS spectrum of the peptide. The stars indicate the peak for the peptide product and its identified masses.

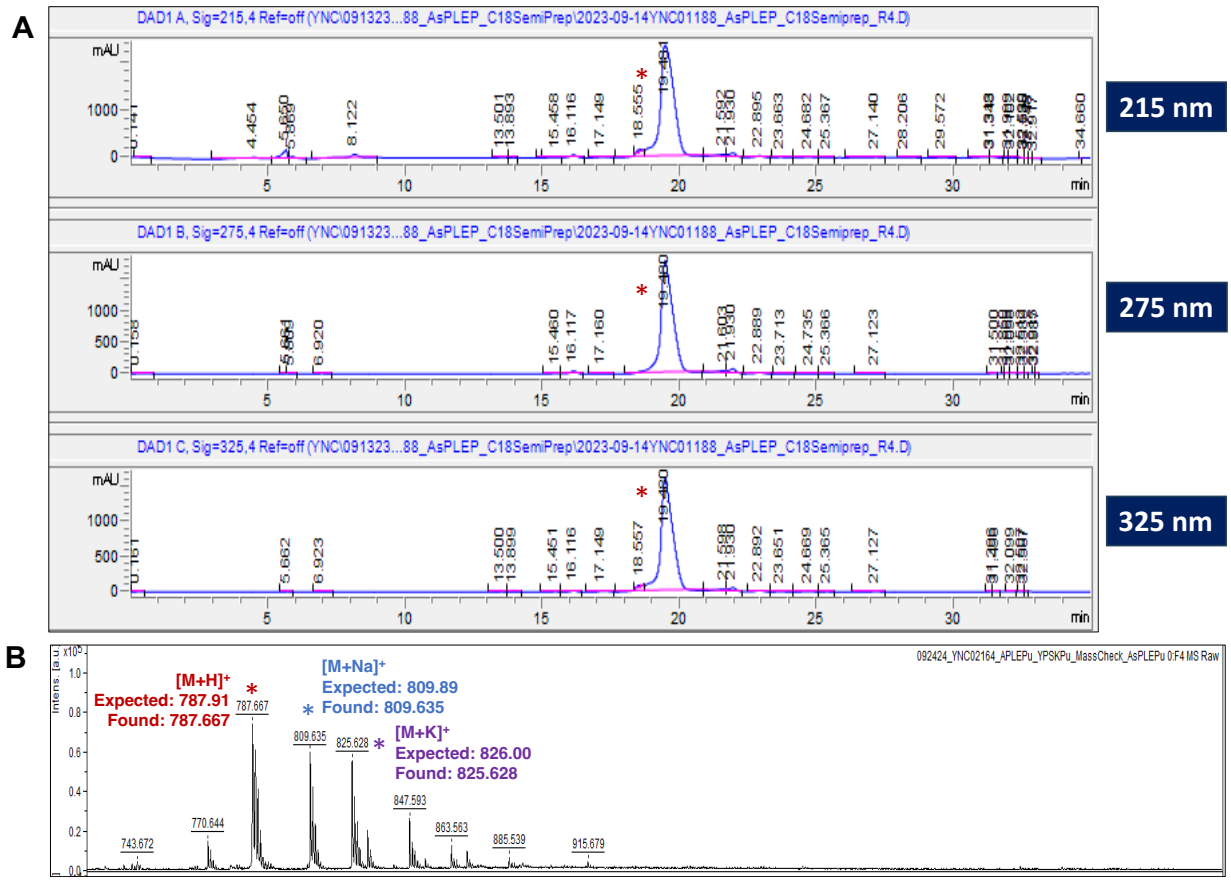


**Figure S10.** Purification and Characterization of A$^{S}$PLEPμ Peptide. (A) HPLC chromatogram of crude peptide sample; different wavelengths were monitored - 215 nm, 275 nm, and 325 nm. (B) MALDI-TOF MS spectrum of the peptide. The stars indicate the peak for the peptide product and its identified masses.

### 3. DPP-4 Proteolysis Assays with Full-Length NPY Peptides (HPLC)

A 19 µL solution of 105.3 µM peptide in DPBS and 26.3 µM Trp internal standard was incubated at 37 °C in the presence of 1 µL of 25 ng/µL DPP-4 (Sigma Aldrich, D3446), to a final concentration of 100 µM peptide, 25 µM Trp, and 1.25 ng/µL DPP-4. After incubating for the desired time (for all-amide t = 0, 2, 5, 8, and 12 minutes), the reaction was then quenched with 2 µL of 1 M hydrochloric acid (HCl). For the thioamide peptides, assays were done with longer incubation time: $NPY_{1\text{-}36}\text{-}Y^{S}{}_{1}$ (t = 0, 5, 10, 20, and 30 minutes) and $NPY_{1\text{-}36}\text{-}P^{S}{}_{2}$ (t = 0, 1, 4, and 24 hours). To prepare samples for analysis with analytical HPLC, the reaction was diluted to 200 µL with Milli-Q. Samples were run in triplicate for each time point. All samples were analyzed by an Agilent 1260 Infinity II series Analytical HPLC using a Phenomenex Luna C8(2) Analytical column (Torrance, CA, USA) (**Figures S11 – S13**). All peptides were monitored at 280 nm and the amount of intact peptide was quantified by integrating peak areas. To determine the percent intact peptide in each sample, the internal standard was used for normalization of the amount of intact peptide; the average ratio of intact peptide from the three trials to internal standard was then compared to the ratio at t = 0 minutes. MALDI-MS was used to confirm the identity of the intact peptide and its cleavage products (**Figures S11 – S13**). A Phenomenex Luna® Omega 5 µm PS C18 100 Å analytical HPLC column was used to analyze all samples (Solvent A: 0.1% TFA in Milli-Q water; Solvent B: 0.1% TFA in acetonitrile).

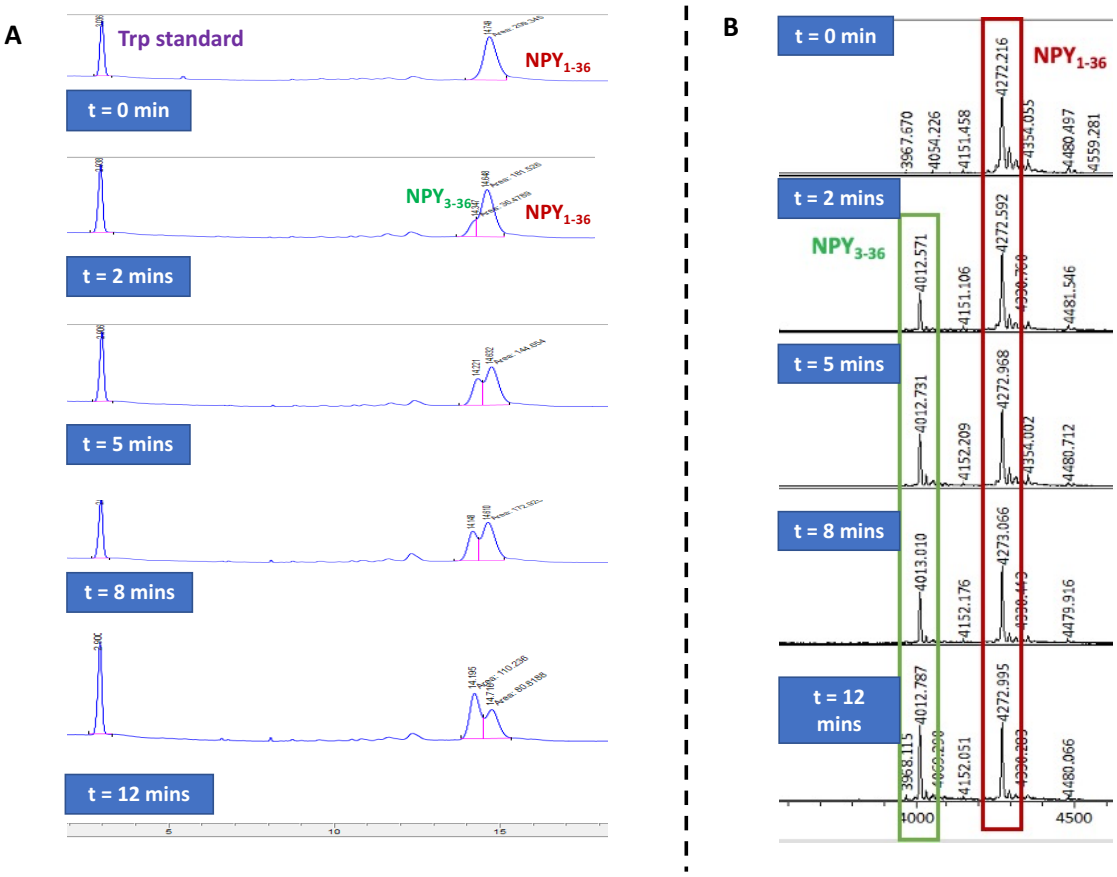


**Figure S11.** DPP-4 Proteolysis Assay with all-amide, full-length $NPY_{1-36}$. (A) Analytical HPLC traces and (B) MALDI at different time points. Expected $[M+H]^+$ for $NPY_{1-36}$ = 4271.08 (found masses indicated with the red box); Expected $[M+H]^+$ for $NPY_{3-36}$ = 4010.96 (found masses indicated with the green box).

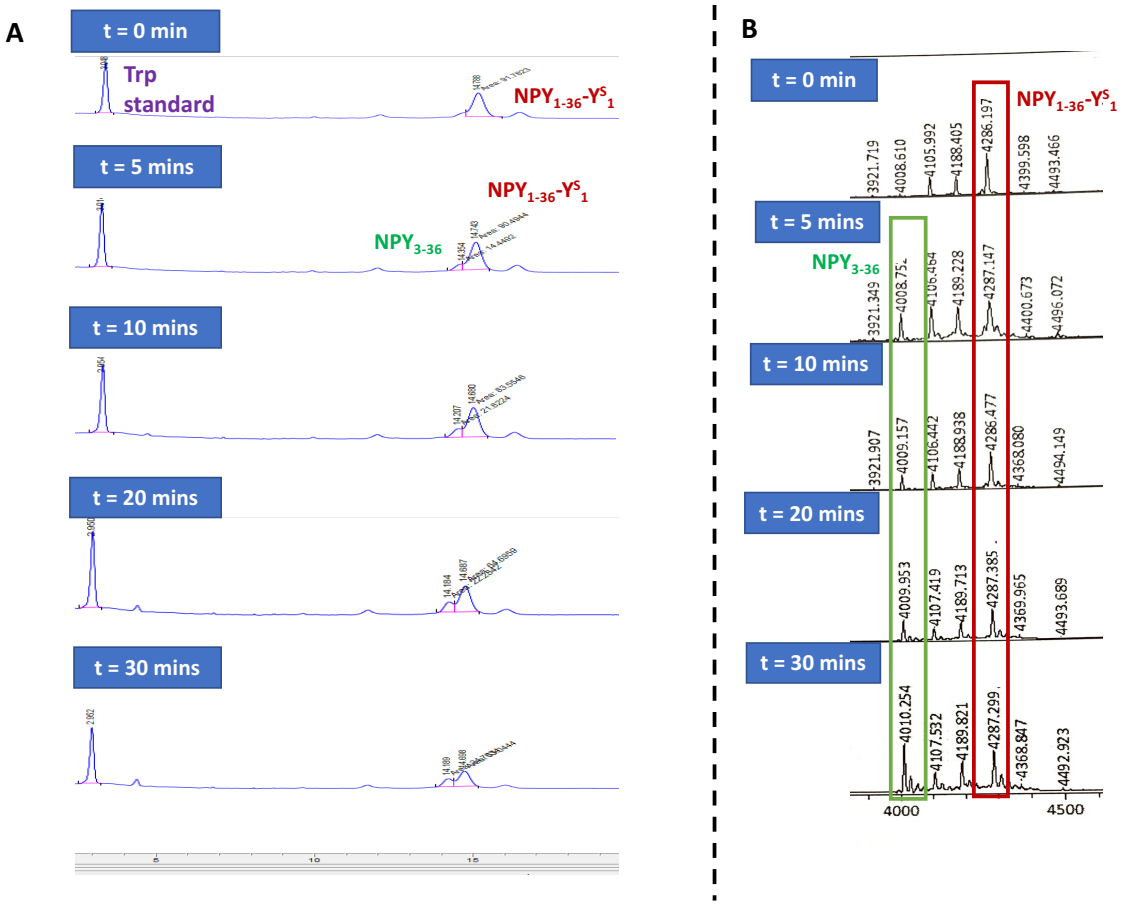


**Figure S12.** DPP-4 Proteolysis Assay with P2 thioamide, full-length $NPY_{1-36}$-$Y^{S}_{1}$. (A) Analytical HPLC traces and (B) MALDI at different time points. Expected $[M+H]^+$ for $NPY_{1-36}$ = 4287.05 (found masses indicated with the red box); Expected $[M+H]^+$ for $NPY_{3-36}$ = 4010.96 (found masses indicated with red box).

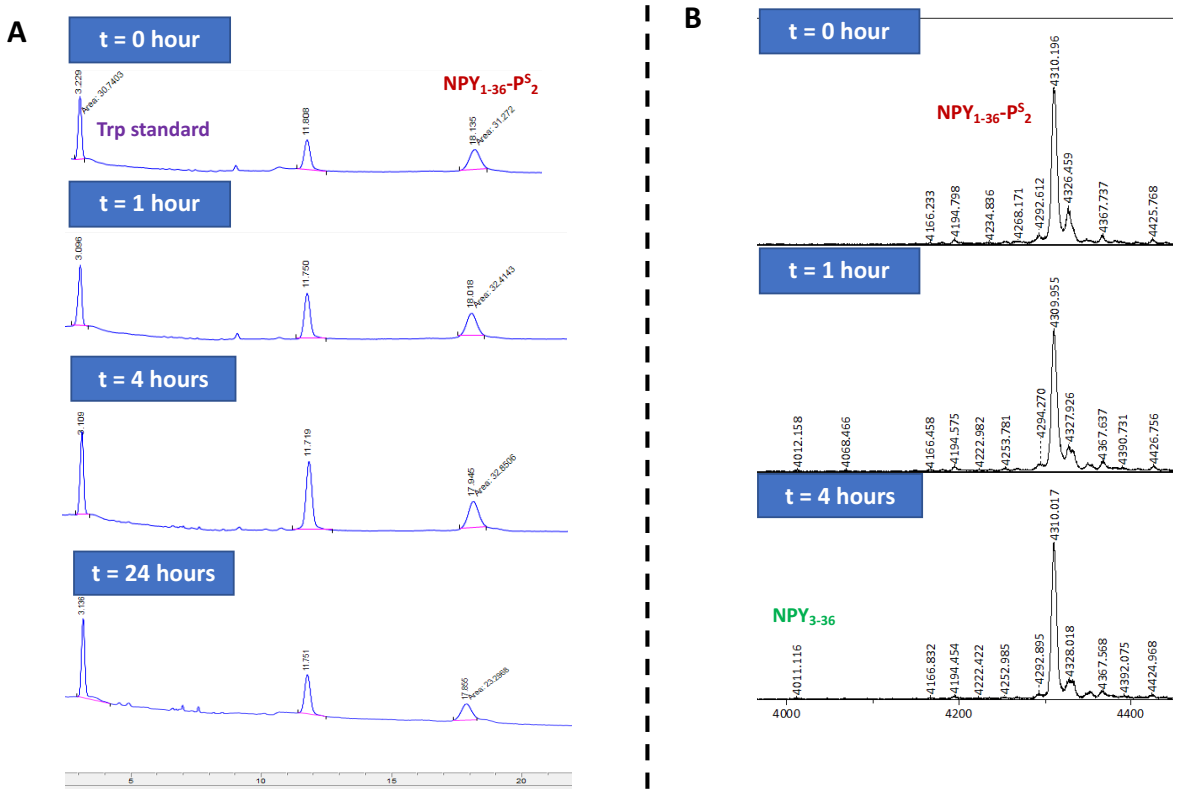


**Figure S13.** DPP-4 Proteolysis Assay with P1 thioamide, full-length $NPY_{1\text{-}36}\text{-}P^{S}_{2}$. (A) Analytical HPLC traces and (B) MALDI at different time points. Expected $[M+H]^{+}$ for $NPY_{1\text{-}36}$ = 4287.05; Expected $[M+H]^{+}$ for $NPY_{3\text{-}36}$ = 4010.96.

## 4. DPP-4 Proteolysis Assays (Steady State Assays)

A 19 μL solution of 5.3 μM peptide was incubated in the absence or presence of 1 μL of 46.2 ng/μL DPP-4 (Sigma Aldrich, D3446), to final concentrations of 5 μM peptide and 2.31 ng/μL DPP-4 in DPBS buffer and pH 7.6 at 27°C. For the PP-based probes (APLEPμ & A$^{S}$PLEPμ), additional assays were conducted at higher DPP-4 concentration of 4.62 ng/μL to improve the cleavage rate and kinetics of the thioamide probes (**Figure S17B**). For the μ-tagged probes, the fluorescence was monitored as a function of time at 390 nm with an excitation wavelength of 325 nm on the Tecan M1000 plate reader. Three replicates were performed for each assay to ensure reproducibility. These primary data are shown. At the end of the plate-reader assay, the sample was diluted to a final volume of 170 μL for validation with HPLC. MALDI MS & HPLC analysis of peptide proteolysis by DPP-4 were also done to confirm the cleavage sites, indicated by the slashes (*e.g.* YP/SKPμ) as summarized in **Figures S14-S17**, and **Tables S4-S7**. A Phenomenex Luna® Omega 5 μm PS C18 100 Å analytical HPLC column was used to analyze all samples using the same gradient of 20-25 % B over 35 minutes (Solvent A: 0.1% TFA in Milli-Q water; Solvent B: 0.1% TFA in acetonitrile).

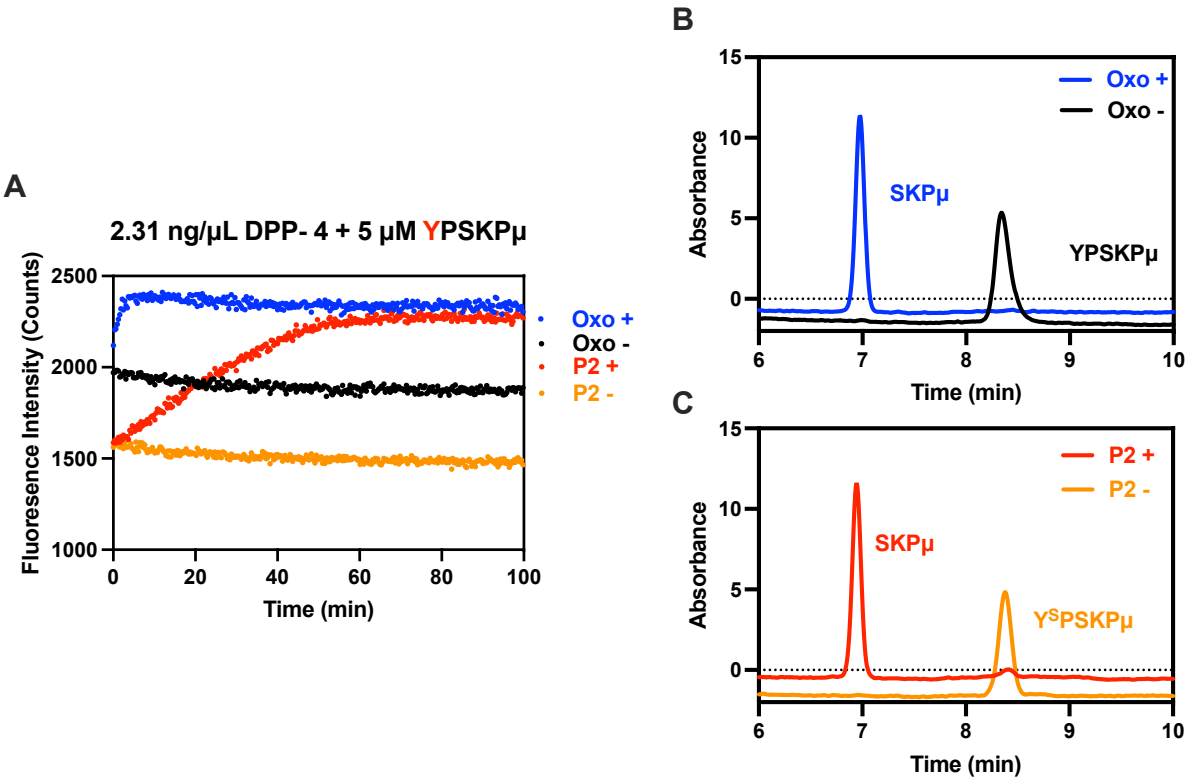


**Figure S14**. DPP-4 Proteolysis of NPY-based Probes (YPSKPµ and Y$^{S}$PSKPµ). (A) Raw fluorescence traces. Fluorescence turn-on by both an all-amide (in the presence of the intrinsic Y-µ quenching) and a P2 thioamide sensor can be used to monitor DPP-4 cleavage. The (-) indicates in the absence of the protease and the (+) indicates the presence of the protease. The fluorescence was monitored as a function of time at 390 nm with an excitation wavelength of 325 nm. All traces show the average of three replicates. (B) & (C) HPLC analysis of NPY-based probes cleaved by DPP-4. Reaction mixtures from fluorescence assays were analyzed by HPLC at 325 nm after completion of the reactions at the end of the assays.

**Table S4.** Masses Identified from DPP-4 Protease Assays with YPSKPµ and Y$^{S}$PSKPµ probes.

| **Condition** | **Fragment** | **[M+H]$^{+}$** | | **[M+Na]$^{+}$** | | **[M+K]$^{+}$** | |
|---|---|---|---|---|---|---|---|
| | | **Calculated** | **Observed** | **Calculated** | **Observed** | **Calculated** | **Observed** |
| **No protease** ***(Negative Control)*** | YPSKPµ *(Intact peptide)* | 836.39 | 836.224 | 858.37 | 858.207 | 874.34 | 874.180 |
| **+ DPP-4** | SKPµ | 576.26 | 576.158 | 598.24 | 598.123 | 614.21 | - |
| **No protease** | Y$^{S}$PSKPµ *(Intact peptide)* | 852.36 | 852.203 | 874.24 | 874.178 | 890.31 | 890.158 |
| **+ DPP-4** | SKPµ | 576.26 | 576.162 | 598.24 | - | 614.21 | - |

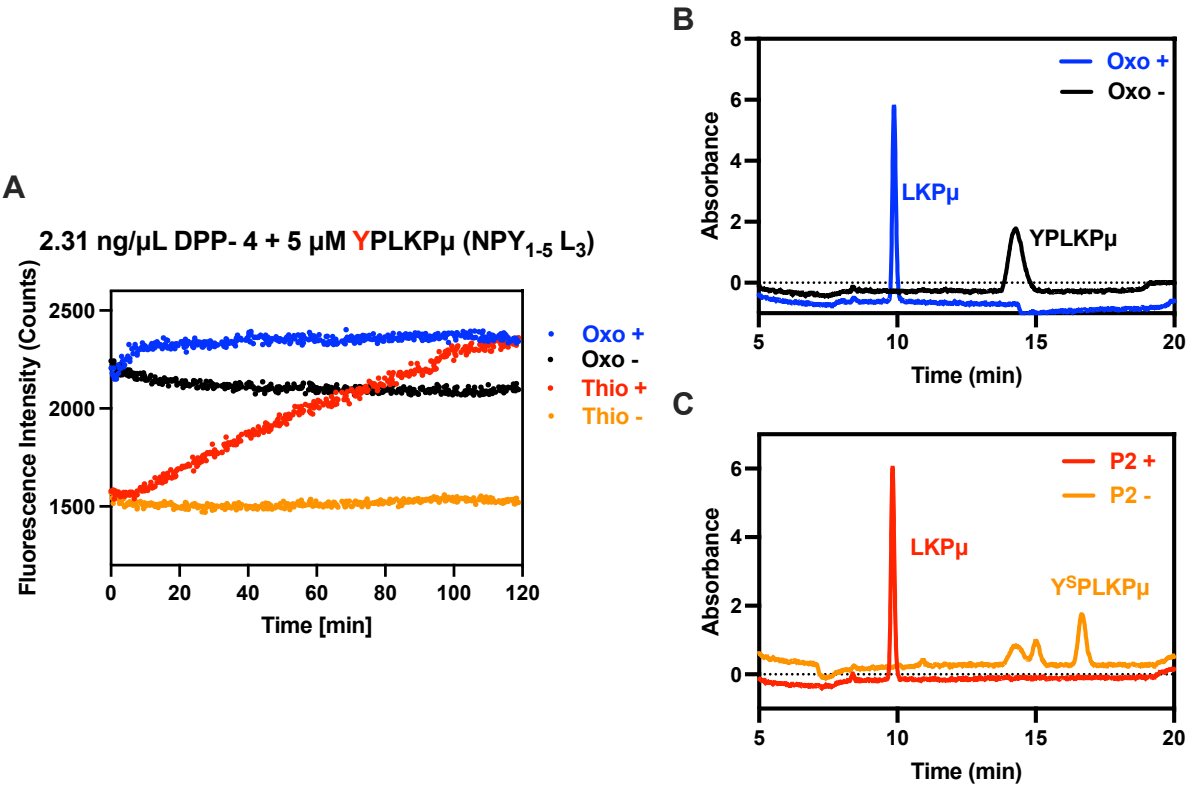


**Figure S15.** DPP-4 Proteolysis of P1' mutated NPY-based probes (YPLKPμ and Y$^{S}$PLKPμ). (A) Raw fluorescence traces. Fluorescence turn-on by both an all-amide (in the presence of the intrinsic Y-μ quenching) and a P2 thioamide sensor can be used to monitor DPP-4 cleavage. The (-) indicates in the absence of the protease and the (+) indicates the presence of the protease. The fluorescence was monitored as a function of time at 390 nm with an excitation wavelength of 325 nm. All traces show the average of three replicates. (B) & (C) HPLC analysis of P1' mutated NPY-based probes cleaved by DPP-4. Reaction mixtures from fluorescence assays were analyzed by HPLC at 325 nm after completion of the reactions at the end of the assays.

**Table S5.** Masses Identified from DPP-4 Protease Assays with YPLKPμ and Y$^{S}$PLKPμ probes.

| Condition | Fragment | $[M+H]^+$ | | $[M+Na]^+$ | | $[M+K]^+$ | |
|---|---|---|---|---|---|---|---|
| | | Calculated | Observed | Calculated | Observed | Calculated | Observed |
| **No protease** ***(Negative Control)*** | YPLKPμ *(Intact peptide)* | 863.00 | 862.542 | 884.98 | 884.488 | 901.09 | 900.785 |
| **+ DPP-4** | LKPμ | 602.71 | 602.352 | 624.69 | 624.484 | 640.80 | 640.518 |
| **No protease** | Y$^{S}$PLKPμ *(Intact peptide)* | 879.06 | 878.728 | 901.04 | 900.749 | 917.15 | 916.382 |
| **+ DPP-4** | LKPμ | 602.71 | 602.471 | 624.69 | 624.407 | 640.80 | - |

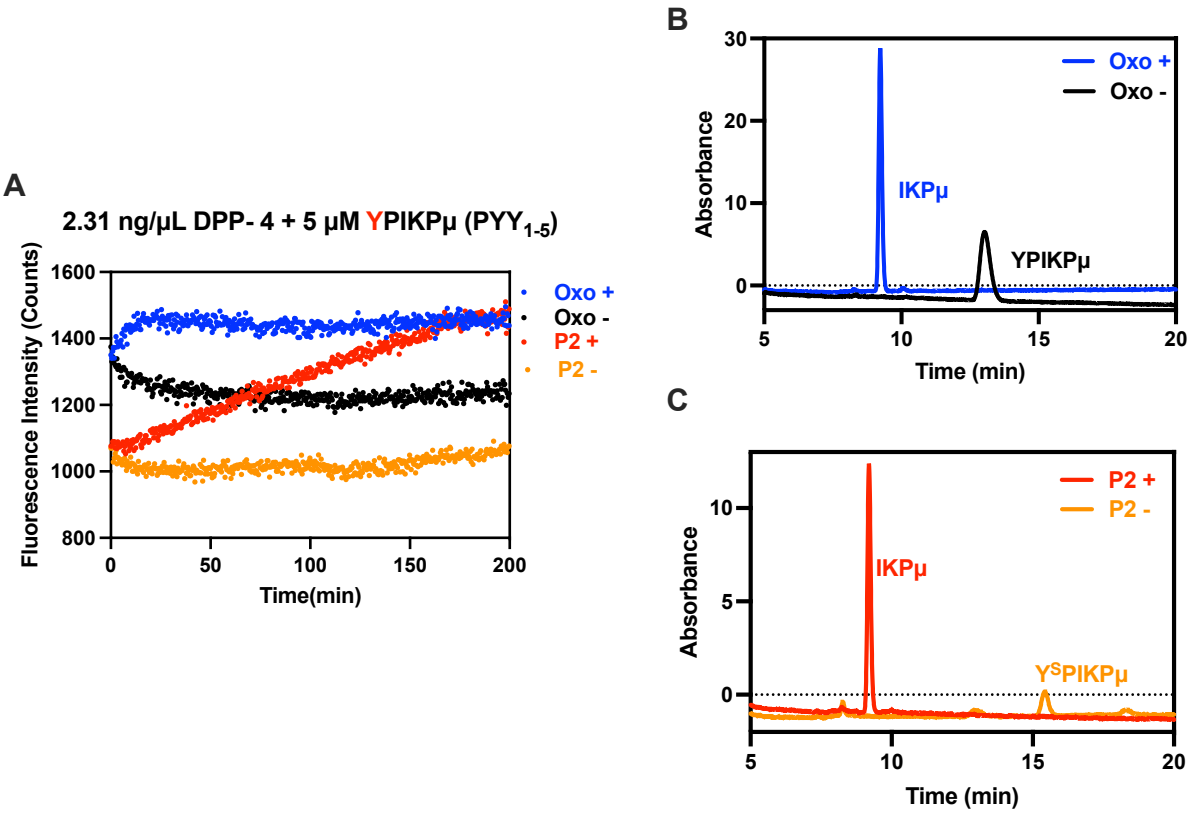


**Figure S16.** DPP-4 Proteolysis of PYY-based probes (YPIKPμ and Y$^{S}$PIKPμ). (A) Raw fluorescence traces. Fluorescence turn-on by both an all-amide (in the presence of the intrinsic Y-μ quenching) and a P2 thioamide sensor can be used to monitor DPP-4 cleavage. The (-) indicates in the absence of the protease and the (+) indicates the presence of the protease. The fluorescence was monitored as a function of time at 390 nm with an excitation wavelength of 325 nm. All traces show the average of three replicates. (B) & (C) HPLC analysis of PYY-based probes cleaved by DPP-4. Reaction mixtures from fluorescence assays were analyzed by HPLC at 325 nm after completion of the reactions at the end of the assays.

**Table S6.** Masses Identified from DPP-4 Protease Assays with YPIKPμ and Y$^{S}$PIKPμ probes.

| Condition | Fragment | $[M+H]^+$ | | $[M+Na]^+$ | | $[M+K]^+$ | |
|---|---|---|---|---|---|---|---|
| | | Calculated | Observed | Calculated | Observed | Calculated | Observed |
| **No protease** ***(Negative Control)*** | YPIKPμ *(Intact peptide)* | 862.44 | 862.124 | 884.42 | 884.320 | 900.39 | 900.088 |
| **+ DPP-4** | IKPμ | 602.32 | 602.039 | 625.70 | 625.528 | 641.28 | - |
| **No protease** | Y$^{S}$PIKPμ *(Intact peptide)* | 878.41 | 878.221 | 900.39 | 900.139 | 916.37 | 916.159 |
| **+ DPP-4** | IKPμ | 602.32 | 602.146 | 625.70 | 625.269 | 641.28 | - |

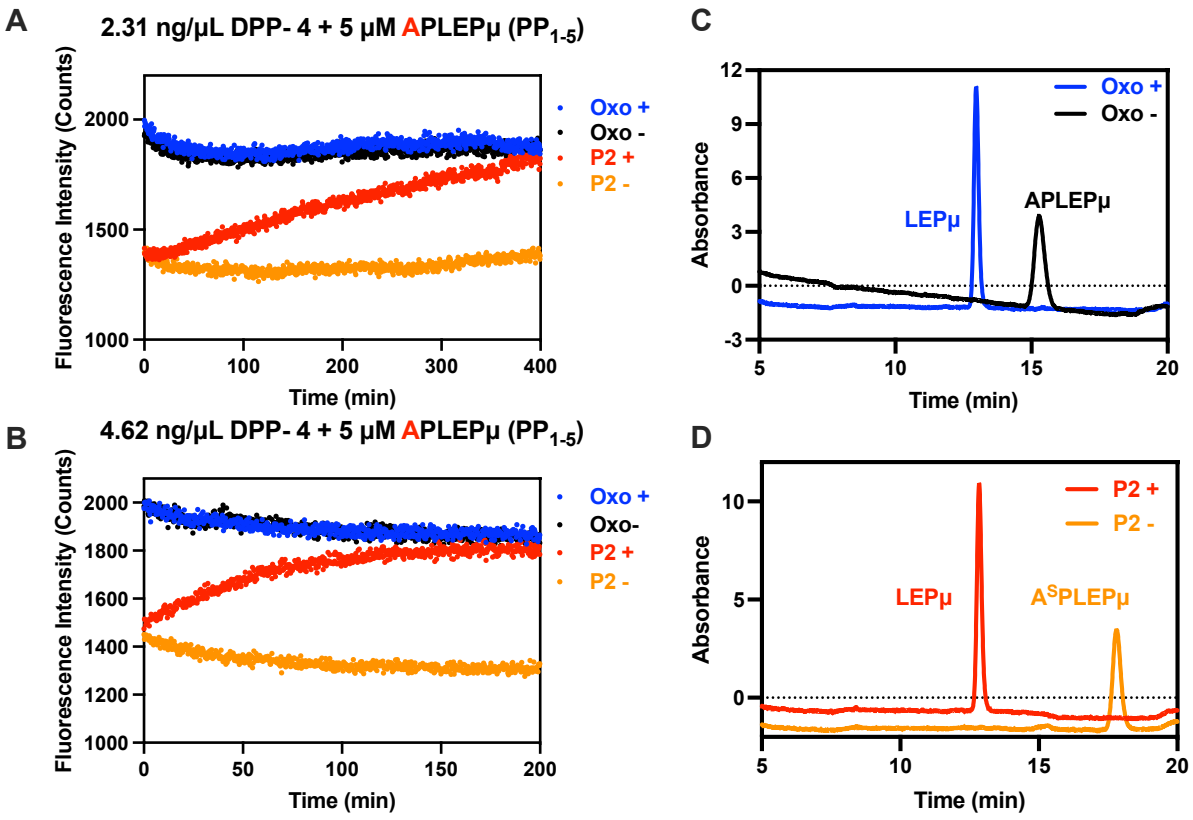


**Figure S17.** DPP-4 Proteolysis of PP-based probes (APLEPμ and A$^{S}$PLEPμ). (A) & (B) Raw fluorescence traces at 2.31 ng/μL DPP-4 and 4.62 ng/μL DPP-4. Fluorescence turn-on by both an all-amide (in the presence of the intrinsic Y-μ quenching) and a P2 thioamide sensor can be used to monitor DPP-4 cleavage. The (-) indicates in the absence of the protease and the (+) indicates the presence of the protease. The fluorescence was monitored as a function of time at 390 nm with an excitation wavelength of 325 nm. All traces show the average of three replicates. (C) & (D) HPLC analysis of PP-based probes cleaved by DPP-4. Reaction mixtures from fluorescence assays were analyzed by HPLC at 325 nm after completion of the reactions at the end of the assays.

**Table S7.** Masses Identified from DPP-4 Protease Assays with APLEPμ and A$^{S}$PLEPμ probes.

| Condition | Fragment | $[M+H]^+$ | | $[M+Na]^+$ | | $[M+K]^+$ | |
|---|---|---|---|---|---|---|---|
| | | Calculated | Observed | Calculated | Observed | Calculated | Observed |
| **No protease** ***(Negative Control)*** | APLEPμ *(Intact peptide)* | 771.85 | 770.354 | 793.83 | 793.404 | 809.94 | 809.385 |
| **+ DPP-4** | LEPμ | 603.27 | 603.330 | 625.63 | 625.320 | 641.74 | 641.296 |
| **No protease** | A$^{S}$PLEPμ *(Intact peptide)* | 787.91 | 786.332 | 809.89 | 809.389 | 826.00 | 825.247 |
| **+ DPP-4** | LEPμ | 603.27 | 602.264 | 625.63 | 625.323 | 641.74 | 641.358 |

## 5. Sitagliptin Inhibition of DPP-4

The same protocol as the above DPP-4 proteolysis assays was used, except that the DPP-4 protease was pre-incubated either with or without sitagliptin (DPP-4 specific inhibitor, ≥98% by HPLC; Sigma-Aldrich SML3205) for 10 minutes before being added to the well containing the probe for the reactions. The data for the all-amide version of the PP-based probe (APLEPμ) was not included since there was no change in fluorescence intensity in the presence and the absence of the protease, as established in the previous assay (**Figure S17**). Sitagliptin is a DPP-4 inhibitor and has $IC_{50}$ value of 18 nM. The final concentration of the inhibitor in the assays were 50 nM. That data for all the probes were shown in **Figure S19**. We also conducted the inhibition assays for the thioamide probes at the higher concentration of the inhibitor of 500 nM (**Figure S20**). We also did a test assay with the commercial DPP-4 probe GP-AMC (H-Gly-Pro-AMC; Anaspec AS-24098), in the absence and presence of sitagliptin, at the same final concentrations of 5 μM probe peptide, 2.31 ng/μL DPP-4, and with or without 50 nM sitagliptin in DPBS buffer and pH 7.6 at 27 °C. The assay with the commercial probe GP-AMC was monitored on the plate reader at the excitation wavelength of 380 nm and emission wavelength of 460 nm (**Figure S18**).

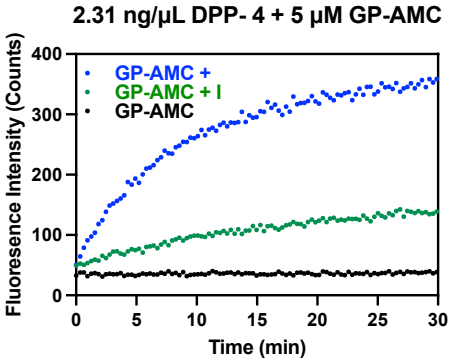


**Figure S18.** Commercial probe GP-AMC Cleaved by DPP-4 in the Presence of Absence of the Inhibitor Sitagliptin. The assays were done with the protease (+), with the protease & 50 nM of the inhibitor (+ I), and without both the protease and inhibitor (negative control; -). Fluorescence intensity was measured at 460 nm. All traces show the average of three replicates.

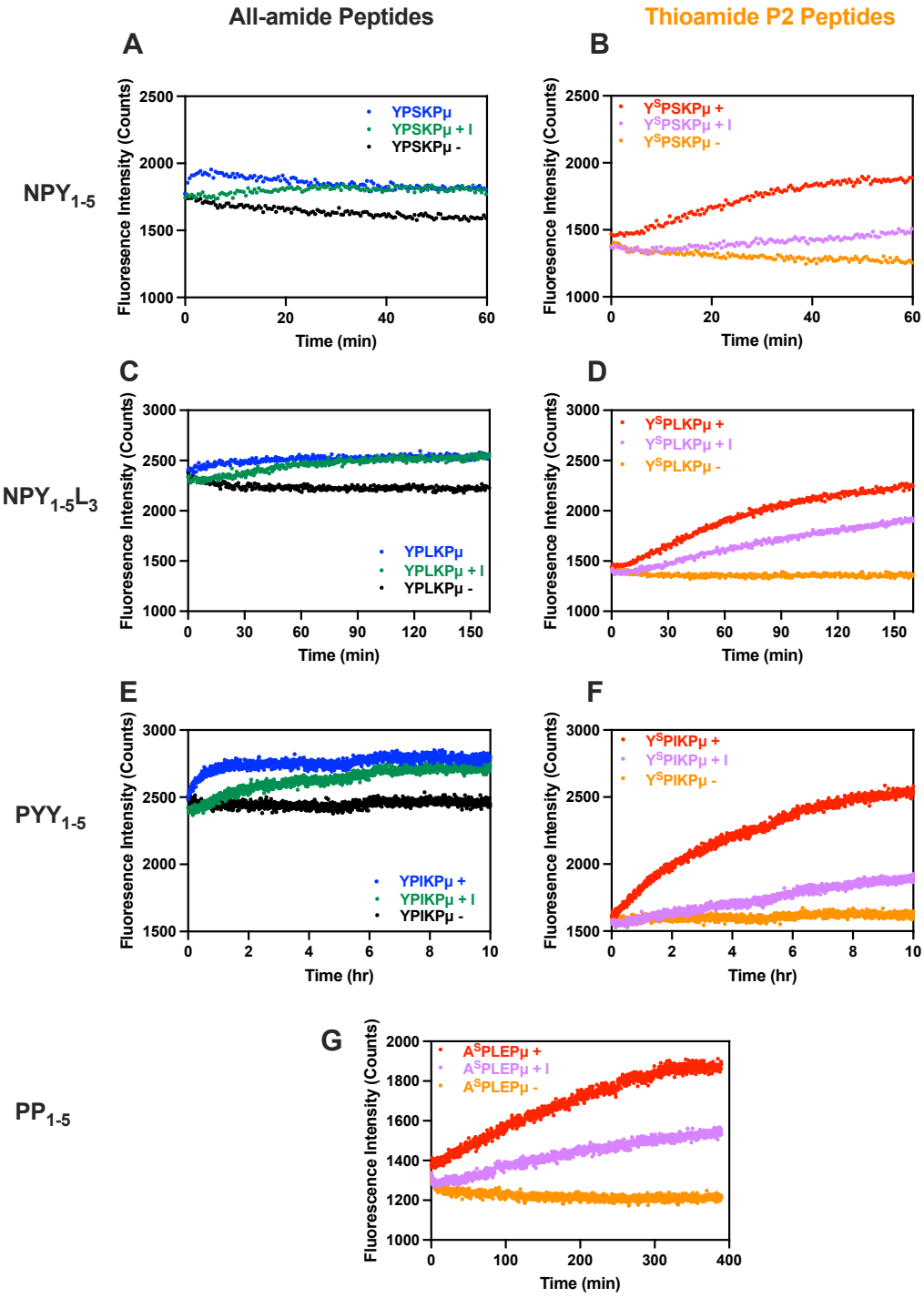


**Figure S19.** DPP-4 Inhibition by Sitagliptin Detected by Our Probes. For each protease, the assays were done with the protease (+), with the protease & 50 nM of the inhibitor (+ I), and without both the protease and inhibitor (negative control; -). Fluorescence intensity was measured at 325 nm. The fluorescence traces are shown for the probes: (A) & (B) NPY-based Probes (YPSKPμ & $Y^{S}$PSKPμ); (C) & (D) NPY-based Probes - P1'mutated (YPLKPμ & $Y^{S}$PLKPμ); (E) & (F) PYY-based probes (YPIKPμ & $Y^{S}$PIKPμ); (G) PP-based probe ($A^{S}$PLEPμ). All probes showed inhibition by sitagliptin, a specific inhibitor of DPP-4. All traces show the average of three replicates.

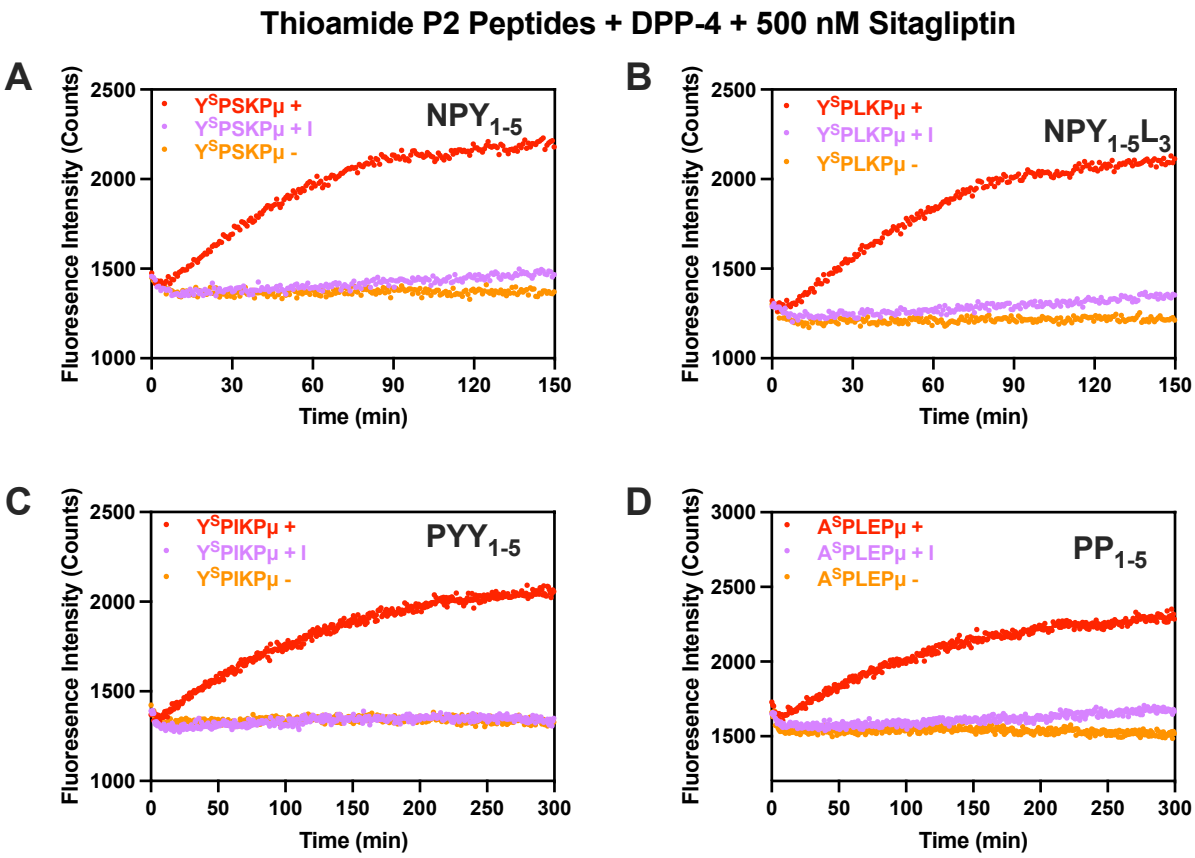


**Figure S20.** DPP-4 Inhibition by Sitagliptin Detected by Our Probes. For each protease, the assays were done with the protease (+), with the protease & 500 nM of the inhibitor (+ I), and without both the protease and inhibitor (negative control; -). Fluorescence intensity was measured at 325 nm. The fluorescence traces are shown for the probes: (A) NPY-based Thioamide Probe ($Y^SPSKP\mu$); (B) NPY-based Thioamide Probe - P1'mutated ($Y^SPLKP\mu$); (C) PYY-based Thioamide probe ($Y^SPIKP\mu$); (G) PP-based probe ($A^SPLEP\mu$). All thioamide probes showed inhibition by 500 nM sitagliptin and more inhibition compared to 50 nM sitagliptin as shown in Figure S19. All traces show the average of three replicates.

## 6. Human Saliva Assays

All assays were conducted with pooled human saliva commercially purchased from Innovative Research (Catalog #IRHUSL5ML). For each probe, 25 µL of human saliva was added to 25 µL of 10 µM probe to a final probe concentration of 5 µM. The probes were diluted in DPBS pH 7.6, and the assays were conducted at 27°C. For the µ-tagged probes, the fluorescence was monitored as a function of time at 390 nm with an excitation wavelength of 325 nm on the Tecan M1000 plate reader. Three replicates were performed for each assay to ensure reproducibility. The primary data are shown in **Figure S22**.

As a control, we conducted a test assay with the commercial DPP-4 probe GP-AMC (H-Gly-Pro-AMC; Anaspec AS-24098) at the same reaction volume and final concentrations 25 µL of 10 µM probe (final probe concentration of 5 µM) and 25 µL human saliva in DPBS buffer and pH 7.6 at 27 °C (**Figure S21**). The assay with the commercial probe GP-AMC was monitored on the plate reader at the excitation wavelength of 380 nm and emission wavelength of 460 nm.

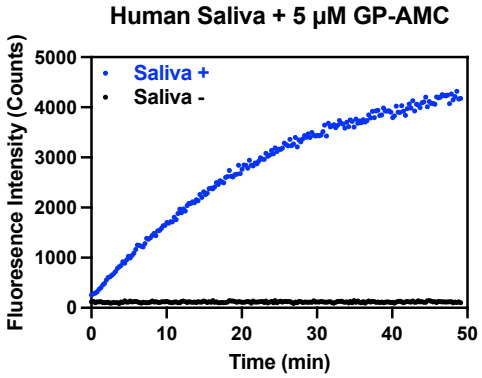


**Figure S21.** Commercial probe GP-AMC Cleaved in the Presence of Human Saliva. The assays were done with the saliva (+) and without the saliva (negative control; -). Fluorescence intensity was measured at 460 nm. All traces show the average of three replicates.

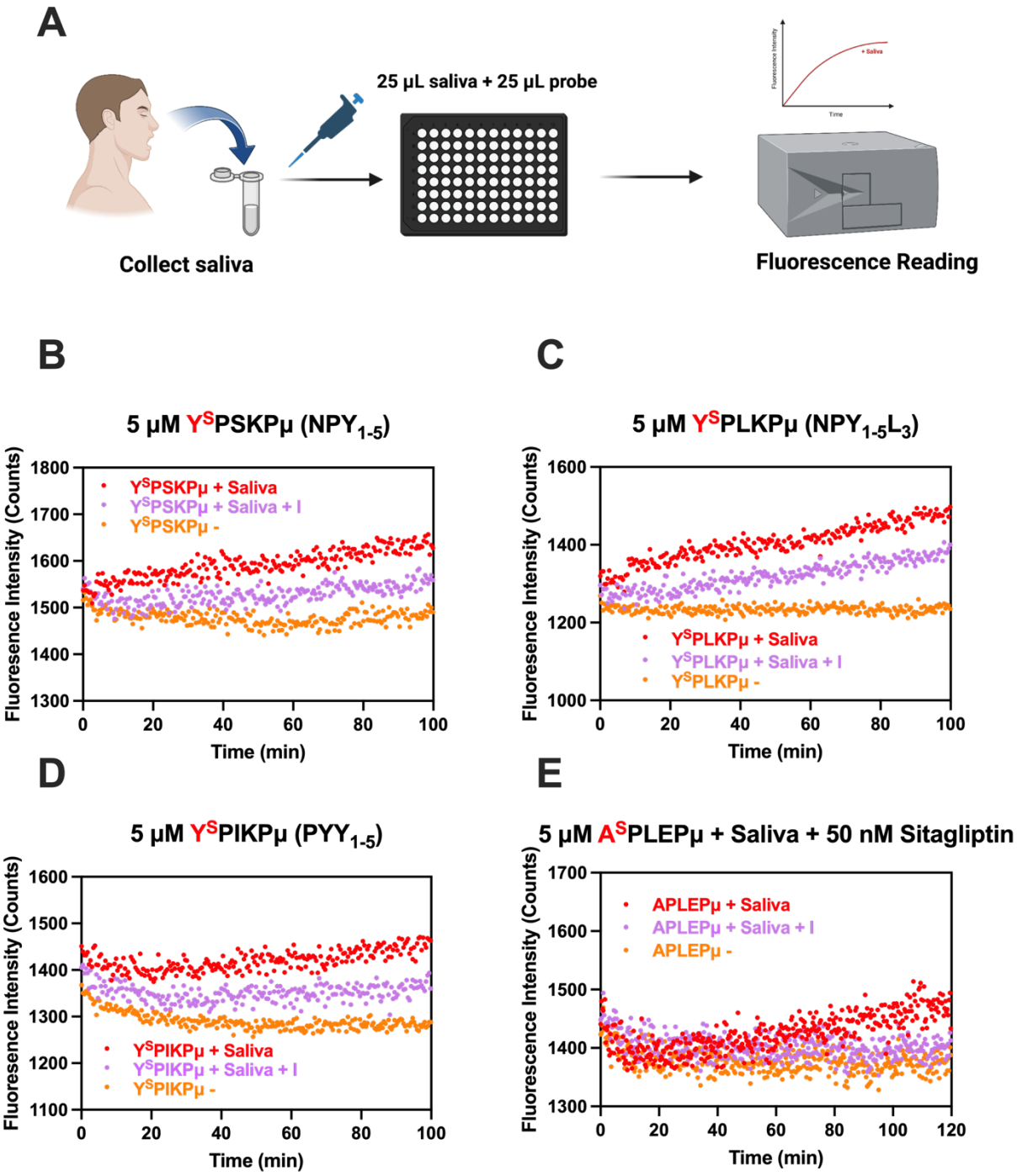


**Figure S22.** DPP-4 detection in human saliva. (A) Work-flow of the saliva assay. Saliva assay with the µ-tagged probes: (B) NPY-based Probes; (C) NPY-based Probes (P1'mutated); (D) PYY-based probes; (E) PP-based probes. For each assay, 25 µL of human saliva was added to 25 µL of 5 µM probe diluted in DPBS. The (-) indicates in the absence of the protease and the (+) indicates the presence of the protease. All traces show the average of three replicates. Figure (A) is created with BioRender.com.

## 7. DPP-4 Inhibition with Sitagliptin in Human Saliva

All assays were conducted with pooled human saliva commercially purchased from Innovative Research (Catalog #IRHUSL5ML). This experiment was done only with thioamide probes. For each probe, 25 μL of human saliva was added to 25 μL of 10 μM probe to a final probe concentration of 5 μM, except for the PP-based probes (15 μM). The probes were diluted in DPBS pH 7.6, and the assays were conducted at 27°C. The same protocol as the above human saliva assays was used, except that the saliva was pre-incubated either with or without sitagliptin (DPP-4 specific inhibitor, ≥98% by HPLC; Sigma-Aldrich SML3205) for 10 minutes before being added to the well containing the probe for the reactions. Sitagliptin is a DPP-4 inhibitor and has $IC_{50}$ value of 18 nM. The final concentration of the inhibitor in the assays were 50 nM. That data for all the probes were shown in **Figure S23**.

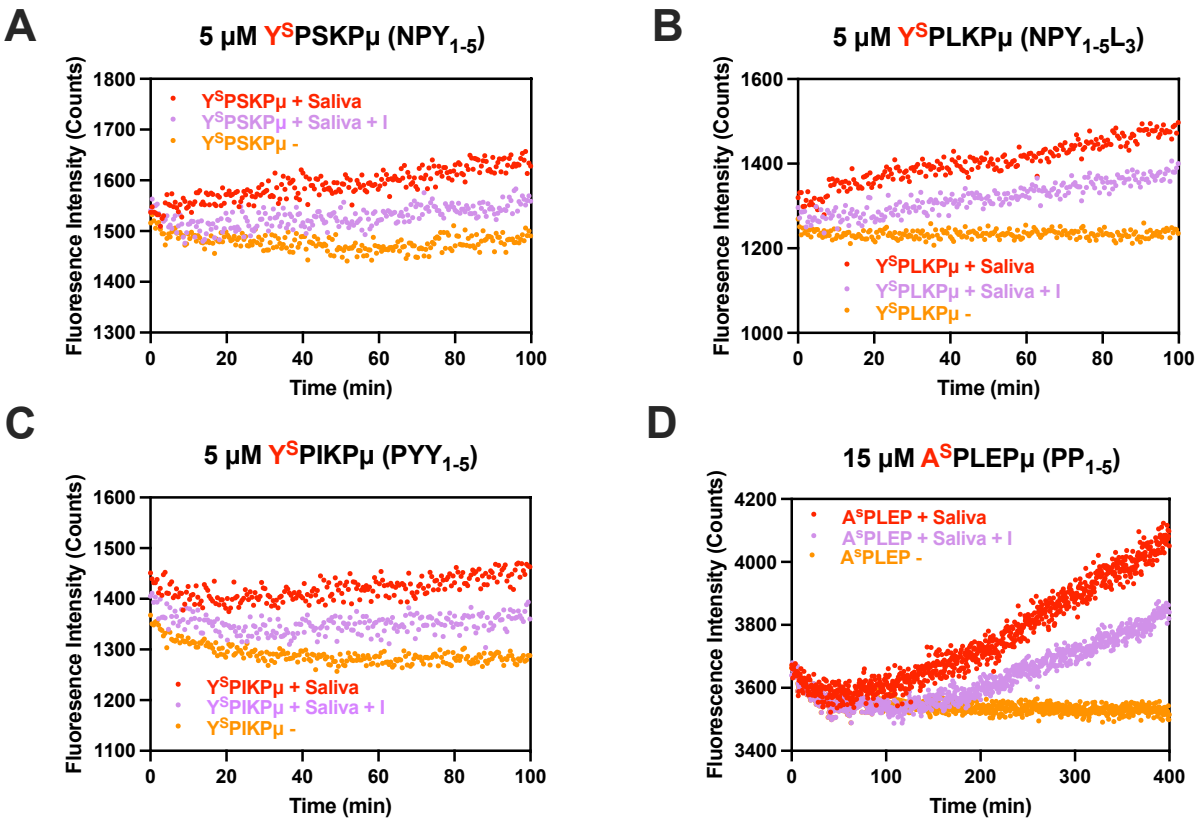


**Figure S23.** DPP-4 Inhibition by Sitagliptin Detected by Our Thioamide Probes in Human Saliva. For each protease, the assays were done with the protease (+), with the protease & 50 nM of the inhibitor (+ I), and without both the protease and inhibitor (negative control; -). Fluorescence intensity was measured at 325 nm. The fluorescence traces are shown for the probes: (A) NPY-based Probes ($Y^{S}$PSKPμ); (B) NPY-based Probes - P1'mutated ($Y^{S}$PLKPμ); (C) PYY-based probes ($Y^{S}$PIKPμ); (D) PP-based probe ($A^{S}$PLEPμ). All probes showed inhibition by sitagliptin, a specific inhibitor of DPP-4. All traces show the average of three replicates.

## 8. Human Saliva Doped with Additional DPP-4

To mimic diseased state biological samples that exhibit elevated DPP-4 level compared to samples from healthy donors, we conducted the assays where human saliva was doped with additional DPP-4 and validated whether if we could discern DPP-4 increase with our probes. All assays were conducted with pooled human saliva commercially purchased from Innovative Research (Catalog #IRHUSL5ML). This experiment was done only with NPY and PP-based thioamide probes. For each probe, 25 µL of human saliva was added to 25 µL of 10 µM NPY-based probe ($Y^{S}$PSKPµ) to a final probe concentration of 5 µM, and 30 µM PP-based probe ($A^{S}$PLEPµ) to a final probe concentration of 15 µM. The probes were diluted in DPBS pH 7.6, and the assays were conducted at 27°C. The same protocol as the above human saliva assays was used, except that additional two different concentrations of DPP-4 were added to the human saliva (the final concentrations of the DPP-4 were 500 ng/mL and 250 ng/mL). In addition, human saliva was pre-incubated either with or without sitagliptin (DPP-4 specific inhibitor, ≥98% by HPLC; Sigma-Aldrich SML3205) for 10 minutes before being added to the well containing the probe for the reactions. The final concentration of the inhibitor in the assays was 500 nM. The data for all the probes were shown in **Figure S24**.

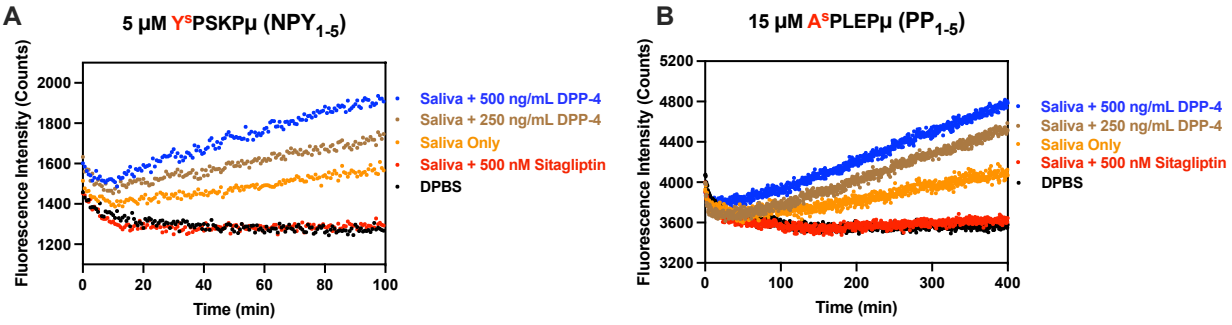


**Figure S24.** Measurement of DPP-4 level in human saliva with thioamide $NPY_{1-5}$ and $PP_{1-5}$ based probes. (A) Thioamide NPY-based probe ($Y^{S}$PSKPµ) or (B) Thioamide PP-based probe ($A^{S}$PLEPµ) was incubated with human saliva in the absence of or in the presence of additional DPP-4. In the presence of DPP-4 specific inhibitor sitagliptin, there was inhibition of the signal, indicating the specificity of our probe.

## 9. Nuclear Magnetic Resonance (NMR)

To gather more insight regarding the structural characteristic of our probe, we collected the following NMR spectra of the NPY-based all-amide peptide (YPSKPμ): COSY (Correlated Spectroscopy) (**Figure S25**), TOCSY (Total Correlation Spectroscopy) (**Figure S26**), and NOESY (Nuclear Overhayser Effect Spectroscopy) (**Figure S27**). The peptide sample was collected at 5 mM of peptide in 90%$H_2O$/10%$D_2O$ with salt, pH = 6.5 (137 mM NaCl, 8.1 mM $Na_2HPO_4$, 2.7 mM KCl, and 1.5 mM $KH_2PO_4$). All spectra were collected with the AVANCE NEO 600 MHz NMR (Bruker). Our results are consistent with previous reports indicating that the C-terminus of NPY is unstructured.[4]

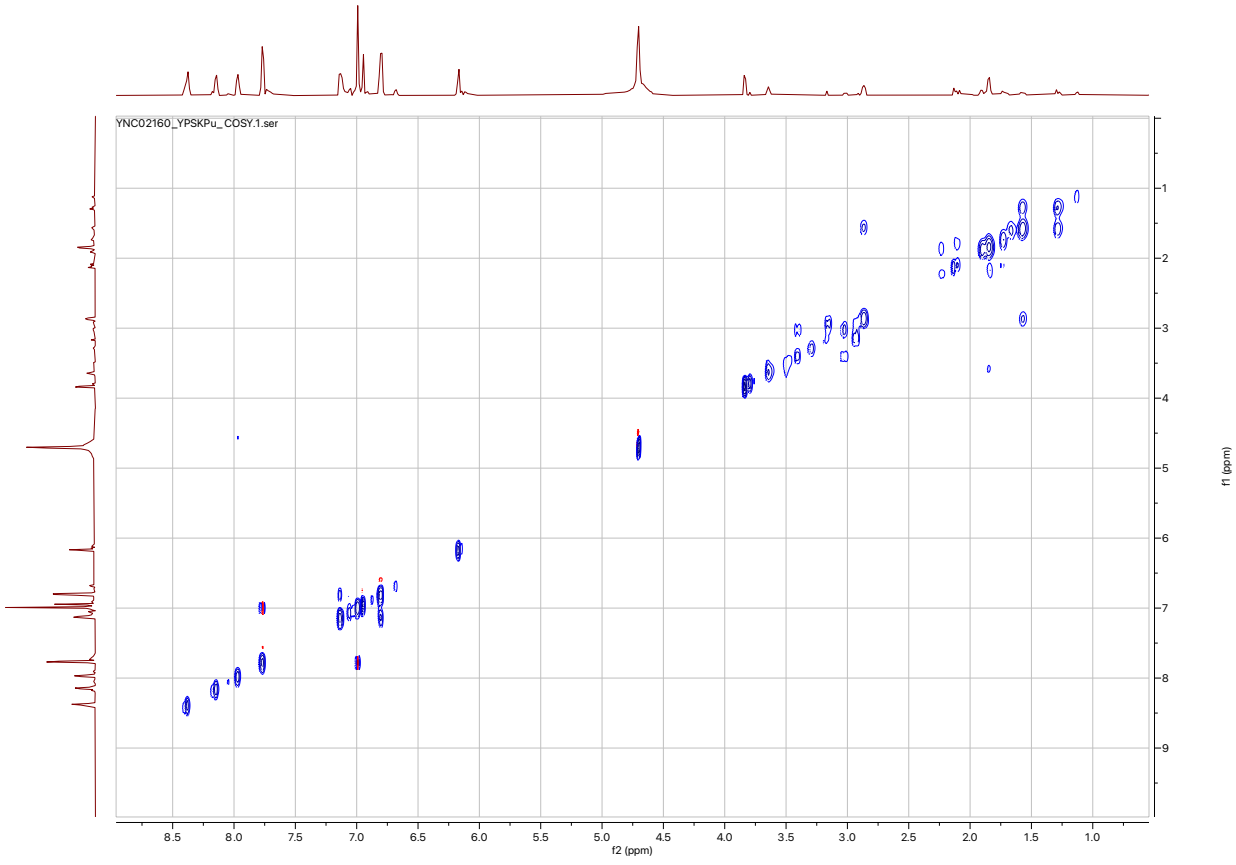


**Figure S25.** COSY of NPY-based peptide probe (YPSKPμ).

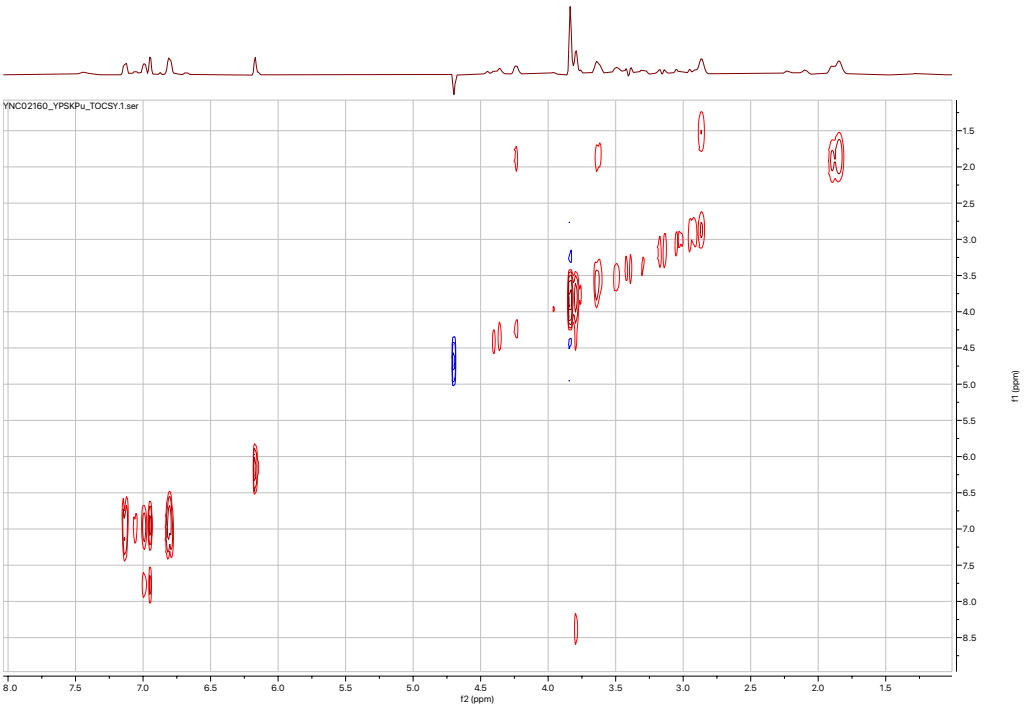


**Figure S26.** TOCSY of NPY-based peptide probe (YPSKPμ).

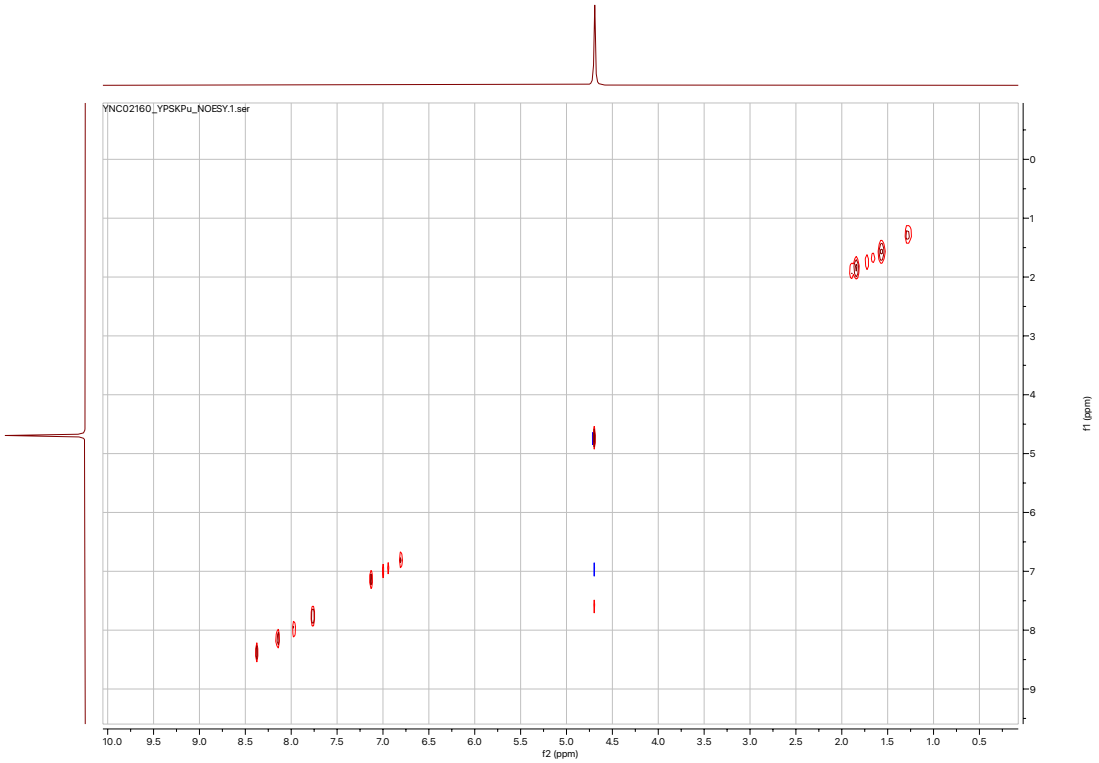


**Figure S27.** NOESY of NPY-based peptide probe (YPSKPμ).

## 10. References

1. T. M. Barrett, X. S. Chen, C. Liu, S. Giannakoulias, H. A. T. Phan, J. Wang, E. K. Keenan, R. J. Karpowicz, Jr. and E. J. Petersson, *ACS Chem Biol*, 2020, **15**, 774-779.
2. C. Liu, T. M. Barrett, X. Chen, J. J. Ferrie and E. J. Petersson, *ChemBioChem*, 2019, **20**, 2059-2062.
3. D. M. Szantai-Kis, C. R. Walters, T. M. Barrett, E. M. Hoang and E. J. Petersson, *Synlett*, 2017, **28**, 1789-1794.
4. V. Saudek and J. T. Pelton, *Biochemistry*, 1990, **29**, 4509-4515.